630

UCRL 5626

MASTER

UNIVERSITY OF CALIFORNIA

Ernest O. Lawrence

Radiation Laboratory

UNDERGROUND NUCLEAR DETONATIONS

LIVERMORE SITE

DISCLAIMER

UCRL-5626

UNIVERSITY OF CALIFORNIA
Lawrence Radiation Laboratory
Livermore, California

Contract No. W-7405-eng-48

UNDERGROUND NUCLEAR DETONATIONS

G. W. Johnson, G. H. Higgins, and C. E. Violet

July 8, 1959

Printed for the U.S. Atomic Energy Commission

UNDERGROUND NUCLEAR DETONATIONS*

G.W. Johnson, G.H. Higgins, and C.E. Violet

Lawrence Radiation Laboratory, University of California
Livermore, California

July 8, 1959

Summary

Since 1952 eight nuclear explosions have been fired underground at the Atomic Energy Commission's Nevada Test Site. The explosions have varied in energy release from 55 tons to 19,000 tons of TNT equivalent and were carried out at depths varying from shallow burial to produce cratering to those depths at which no visible effects appeared on the surface. The major experimental data from these explosions, as well as the phenomenology of the deeper shots, is summarized here.

1. Introduction

During the 1955 nuclear weapons test series in Nevada it became increasingly clear to the Lawrence Radiation Laboratory that concern over fallout would be a serious limitation on future weapons tests. Therefore, based on a suggestion of Griggs and Teller [1956], consideration was given to the possibility of testing underground at such depths that there would be no escape of radioactivity to the atmosphere. Further detailed consideration led to the design of an experiment, code-named Rainier, to test the feasibility of containment of the radioactive debris from a nuclear explosion. This experiment conducted on September 19, 1957 was completely successful and all objectives of the experiment were achieved. The results of this 1.7-kiloton detonation have been previously reported in considerable detail [Johnson and others 1958, Johnson and Violet 1958, Diment and others 1959]. Its continued study has led to a fairly complete understanding of the physical and chemical processes associated with underground nuclear explosions. Subsequent to the Rainier detonation, five additional nuclear devices were fired underground at the Nevada Test Site during October 1958 in connection with

* Work was performed under the auspices of the U.S. Atomic Energy Commission.

weapon development programs. The preliminary results of these later explosions have been published [Johnson and Violet 1958].

In this paper all major results presently available from these shots, as well as three earlier cratering shots, are summarized and the phenomenology of these events is discussed.

2. Experimental Conditions

All of the explosions, except the earlier cratering shots, took place in a thick formation of bedded tuffs. The three exceptions, which were detonated in a lightly cemented alluvium, will not be described in detail but are included for completeness. The coordinates and time of detonation for each explosion are listed in Table 1.

TABLE 1

List of Events, Dates, Times and Locations

Event	Date	Time Z	Latitude ° ' "	Longitude ° ' "	Elevation ft
Jangle-S	19 Nov. 51	1659:59.72	37 07 54 N	116 02 19 W	4214
Jangle-U	29 Nov. 51	1959:59.72	37 10 11 N	116 02 33 W	4298
Teapot-Ess	23 Mar. 55	2030:00.01	37 10 06 N	116 02 38 W	4226
Neptune	14 Oct. 58	1800:00.15	37 11 37.88 N	116 11 58.88 W	6716
Blanca	30 Oct. 58	1500:00.15	37 11 09.36 N	116 12 07.28 W	6138
Logan	16 Oct. 58	0600:00.140	37 11 03.03 N	116 12 04.04 W	6141
Rainier	19 Sept. 57	1659:59.454	37 11 44.800 N	116 12 11.35 W	6615
Tamalpais	8 Oct. 58	2200:00.131	37 11 43.10 N	116 12 01.64 W	6616
Evans	29 Oct. 58	0000:00.15	37 11 41.46 N	116 12 17.03 W	6620

The geological structure in which the deep shots took place is characterized by 250 feet of welded tuff under which is 1700 feet of bedded tuffs and a thick bed of dolomite [Diment and others 1958a]. The locations of the several shot points are illustrated in Figure 1. The details of the tunnels and stemming for each event are shown in Figures 1 through 8 of the Appendix. A stratigraphic feature of some importance in interpretation is the loosely consolidated zone in Tos_7, the limits of which are indicated by dashed lines

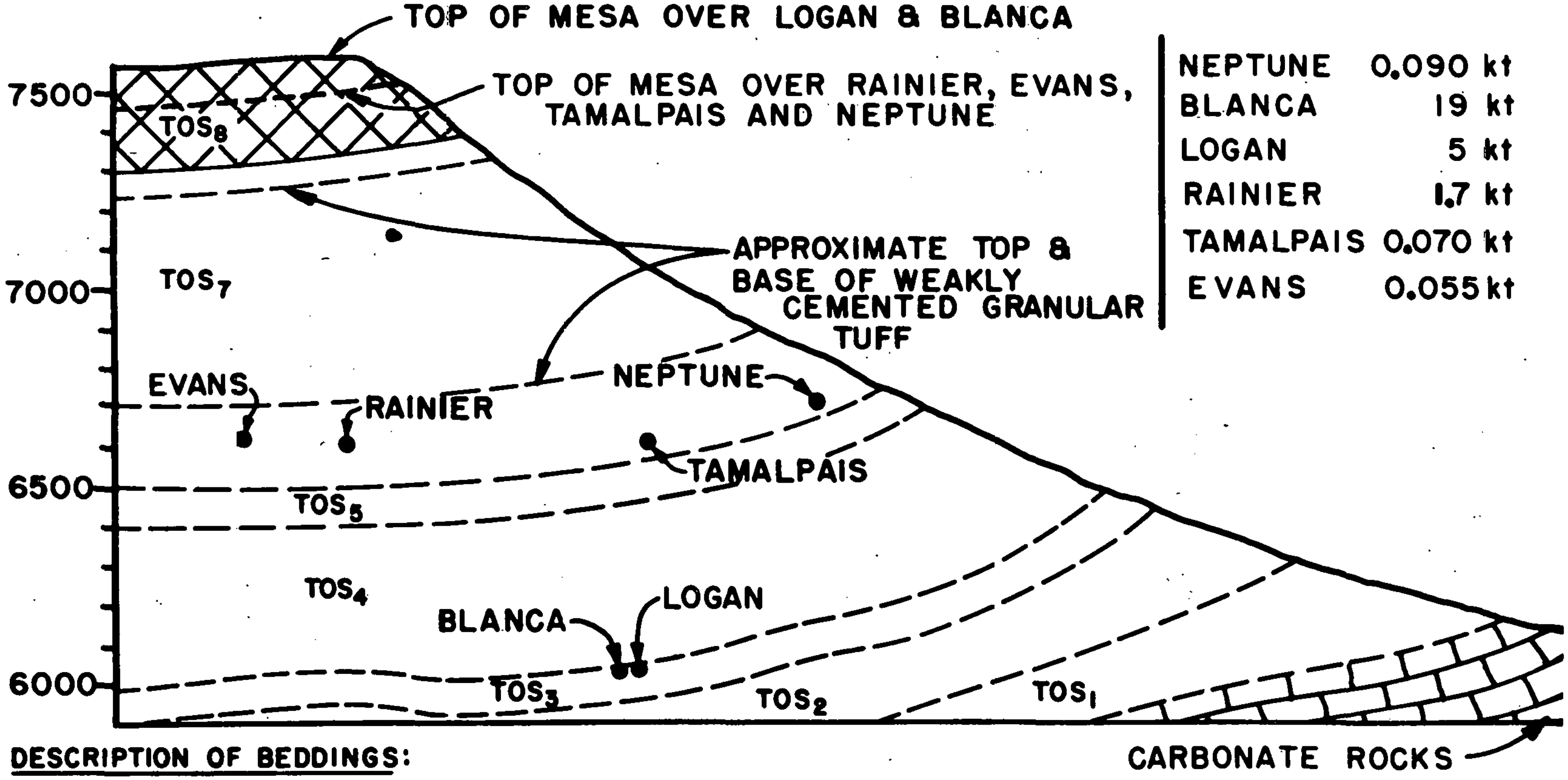

DESCRIPTION OF BEDDINGS:

TOS_8	WELDED TUFF; RHYOLITE TO QUARTZ LATITE.
TOS_7	FRIABLE TUFF; MOSTLY ALL TUFFS ARE LOOSELY CEMENTED AND "SANDED"; LIGHT GRAY TO GRAYISH BROWN.
TOS_5	BEDDED TUFF; WELL CEMENTED; LIGHT YELLOW GREEN.
TOS_4	BEDDED TUFF; WELL CEMENTED, LIGHT GRAY TO BUFF, SOME PINK.
TOS_3	BEDDED TUFF; WELL CEMENTED, RED AT TOP AND BASE, PINK TO BUFF INTERBEDS.
TOS_2	BEDDED TUFF; MOSTLY LIGHT GRAY TO BUFF.
TOS_1	BEDDED TUFF; PURPLISH TO PINKISH RED.

GENERAL NOTE:

1. THE DISTANCE RELATIONSHIPS BETWEEN THE ZERO W.P.'s AND THE PROFILE OF THE MESA, ARE CORRECT; HOWEVER, DUE TO THE COMPOSITE NATURE OF THE PROFILE, THE PROJECTED RELATIVE DISTANCES BETWEEN THE W.P.'s ARE NOT CORRECT.

MUL-7144

Fig. 1. Profile of mesa showing zero sites.

in Figure 1. Rainier, Evans, Tamalpais, and Neptune were detonated in this lithologic unit about 100 feet below this lower limit. Blanca and Logan were detonated in Tos_3 about 600 feet below this limit.

Physical and chemical properties of the medium, averaged in the vicinity of the Logan, Blanca, and Rainier detonation points are listed in Tables 2 through 7.

TABLE 2

Average Values of Density, Porosity and Water Content
(Errors are standard deviations)

	Logan [Diment and others 1958b]	Blanca [USGS 1958]	Rainier [Diment and others 1959]
Dry bulk density (g/cm^3)	1.8±0.3	1.6±0.2	1.7±0.2
Natural state bulk density (g/cm^3)	2.1±0.2	1.9±0.2	2.0±0.2
Grain density (g/cm^3)	2.6±0.1	2.4±0.1	2.3±0.2
Porosity (percent)	30.6±7.4	33.2±6.0	24.4±7.0
Water content (weight percent)	14.5±3.5	17.5±3.5	15.3±3.5

TABLE 3

Average Chemical Composition
(Percent by weight for air-dry samples)

	Location	
	Logan [Diment and others 1958b]	Rainier [Diment and others 1959]
SiO_2	71.5	66.9
Al_2O_3	13.0	12.3
CaO	0.7	2.3
Fe_2O_3	1.8	2.2
MgO	0.4	1.0
Na_2O	1.3	1.3
K_2O	6.6	2.2
H_2O	4.5	10.6
Balance	0.2	1.2

TABLE 4

Mineral Composition by Volume Percent

	Logan and Blanca [USGS 1958]	Rainier [Diment and others 1959]
Phenocrysts	19.4	17.4
Quartz	6.9	2.6
Alkali Feldspar	5.6	6.1
Plagioclase	6.0	6.8
Biotite	0.5	1.3
Pyroxene and Amphibole	---	0.2
Magnetite	0.4	0.4
Xenoliths	1.6	6.7
Shards and Lapilli Matrix	70.7	68.4
Heulandite	not differentiated	23
Montmorillomite	"	12
β - Cristobalite	"	11
Amorphous Material	"	22
Vesicles	8.3	7.5

TABLE 5

Thermal Properties

A. Specific Heat* for Rainier Tuff (cal/gram/°C) [Warner and Violet 1959]

Water content, (grams H_2O/ gram dry sample)	Temperature °C: 25	100	200	400	600
0	0.18	0.21	0.24	0.27	0.30
0.15	0.28	0.31	-	-	-
0.20	0.31	0.33	-	-	-
0.30	0.34	0.36	-	-	-

*Calculated from chemical analysis. Does not include heat of vaporization of water.

(continued)

TABLE 5 (continued)

B. Thermal Conductivity (cal/cm^2/sec/°C/cm) [Diment and others 1958a]

	Rainier	Logan
Dry	0.0011	0.0014
Wet	0.0016	0.0020

C. Melting Range: 850-1500°C

D. Estimated enthalpy to molten state (≈1500°C): 700 cal/g
Estimated enthalpy to vapor state (≈3000°C): 3000 cal/g

TABLE 6

Average Values of Strength and Elastic Properties

A. Static Tensile Properties of Rainier Tuff [Diment and others 1959]

Air Dry Tensile Strength, psi	165
Air Dry Young's Modulus, psi	0.46×10^6
Air Dry Poisson's Ratio	0.12
Calculated Rigidity Modulus, psi	0.22×10^6

B. Static Compressive Properties of Rainier Tuff [Diment and others 1959]

	Air dry	Natural state	Natural state under hydrostatic pressure 1,000 psi
Compressive Strength, psi	4700	1200	5100
Young's Modulus, psi	1.1×10^6	0.18×10^6	0.37×10^6
Poisson's Ratio	0.11		
Calculated Rigidity Modulus, psi	0.50×10^6		

C. Dynamic Properties of Rainier Tuff [Diment and others 1958a]

f_L	f_T	b	v_L	v_T	E $\times10^6$	G $\times10^6$	σ
5900	4000	0.1	7940	5380	1.07	0.49	0.09

where f is resonant frequency, cps.

L and T are longitudinal and torsional modes, respectively.

b is specific damping capacity determined from width of resonance amplitude curve.

(continued)

TABLE 6 (continued)

v is calculated acoustic velocity, ft/sec.
E is calculated Young's modulus, psi.
G is calculated rigidity modulus, psi.
σ is calculated Poisson's ratio.

D. Bulk Modulus of Rainier Tuff, psi [Warner and Violet 1959]

	Unjacketed	Jacketed
Sample water-saturated	5.7×10^6	0.54×10^6
Average oven-dry sample	4.8×10^6	0.41×10^6

TABLE 7

Miscellaneous Properties of Rainier Tuff

A. Porosity at elevated pressures (average of 2 samples of 28% porosity) [Warner and Violet 1959]

Pressure, psi	0	1000	2000	3000	4000
% Reduction in porosity	0	6%	8%	10%	12%

B. Permeability to Air (millidarcies)[Warner and Violet 1959] to Brine (millidarcies).

	Average*	Range**	Average	Range
Rainier	6.0	0.95 - 41	1.4	0.084 - 27
Logan	0.81	0.14 - 2.4	0.036	0.00076 - 0.24

*Averages are computed assuming log-normal distribution.
**Ranges are the total ranges of values observed.

(continued)

TABLE 7 (continued)

C. Seismic Velocity, Vertical Distribution over Rainier [Swift and Sachs 1959]

Interval depth below surface, feet	Interval velocity, ft/sec	Distance above Rainier shot room, feet
230 - 270	7,150	665 - 625
270 - 310	13,700	625 - 585
310 - 395	6,650	585 - 500
395 - 525	7,070	500 - 370
525 - 675	7,180	370 - 220
675 - 775	5,850	220 - 120

(Shot room at depth 895 feet.)

3. General Results

The gross results of the explosions will be described in terms of the visible behavior in the vicinity of the shot point, the escape of radioactivity, the air blast, and the ground shock. The explosions are listed in order of increasing scaled depth in Table 8. The scaled depth is defined as $D/W^{1/3}$, where D is the actual depth in feet and W is the energy release in kilotons (kt) of TNT equivalent. The depth D in the table is the distance to the nearest point on the surface. The column in the table entitled "Measured radioactivity deposited on surface" represents the percentages of the total radioactivity which appeared on the surface, neglecting possible enrichment of particular isotopes.

One kiloton of TNT equivalent is defined as the prompt release of 10^{12} calories of energy (4.2×10^{19} ergs). This energy is determined by multiplying the number of fissions, as measured radiochemically, by the prompt energy release (179 Mev or 2.86×10^{4} ergs per fission). Prompt energy is the sum of the kinetic energy of the fission fragments, and the prompt neutron and prompt gamma ray energies. The delayed energy release due to radioactivity decay amounts to another 22 Mev per fission. About 15 Mev of this energy appears eventually as heat, of which about 7 Mev is released in the first 20 minutes.

TABLE 8

Major Features of Underground Nuclear Explosives

Event	Yield (W) kt	Medium	Depth (D) feet	Scaled Depth $D/W^{1/3}$	Measured radioactivity deposited on surface %	Crater volume yd^3	Crater volume/kt yd^3
Jangle-S	1.2±0.1	Alluvium	-3.5*	-3.3*	>65	1,650	1,400
Jangle-U	1.2±0.1	"	17	16	>80	37,000	31,000
Teapot-Ess	1.2±0.1	"	67	63	90	96,000	80,000
Neptune	0.090±.020	Bedded Tuff	99	220	1-2	33,000	370,000**
Blanca	19.0±1.5	" "	835	310	<0.5	0	0
Logan	$5.0^{+0.2}_{-0.4}$	" "	830	485	0	0	0
Rainier	1.7±0.1	" "	790	670	0	0	0
Tamalpais	0.072±.010	" "	330	780	0+	0	0
Evans	0.055±.030	" "	840	2200	0++	0	0

*3.5 feet above surface.

**This explosion took place in bedded tuff under a sloping surface 1:3 so the crater is probably larger than would be expected on a level surface.

+No breakthrough to surface but radioactive gases in large quantities leaked into the tunnel.

++No breakthrough to surface but stemming failed, releasing gross fission activity into the tunnel.

A. Escape of Radioactivity

In discussing the effectiveness of containment of radioactivity it is necessary to examine not only the escape through the surrounding formation but also the success of the stemming in the tunnels.

For Rainier (1.7 kt) and Logan (5.0 kt) there was no detectable escape of radioactivity to the atmosphere or into the tunnels. From Blanca (19 kt) a chimney developed to the surface and broke out 15 seconds after the detonation. The cloud rose about 1,000 feet and deposited radioactivity on the ground. On integration of the radioactivity in the surveyed area (Figure 9, Appendix) it was found that 0.3 to 0.5% of the gross radioactivity escaped and had been deposited locally. Volatile isotopes were enriched several fold in the vented radioactivity.

The tunnels collapsed at radii of 200 feet (Rainier), 820 feet (Logan), and 850 feet (Blanca) from their respective centers of detonation. There was no detectable leak of radioactivity into the tunnels from any of these explosions. On digging back into the sites it was found that radioactivity had been projected down the tunnels 600 feet for Blanca and 190 feet for Logan.

From this experience it has been demonstrated that the radioactivity released by nuclear explosions can be successfully contained underground. It may be seen from Table 8 that the escape of radioactivity is small at a scaled depth of 300 $W^{1/3}$, and at a scaled depth of 500 $W^{1/3}$ it was not detectable. All radioactivity would probably be contained at a depth of 400 $W^{1/3}$ or greater in tuff.

Neptune, Teapot-Ess, Jangle-U, and Jangle-S, all produced craters and released radioactivity to the atmosphere. In all these cases almost all of the radioactivity that escaped returned to earth within a few miles. With Neptune (Figure 10, Appendix) only 1% of the radioactivity escaped and was deposited near the crater, although the volatile isotopes and those isotopes with gaseous precursors were enriched several fold as noted for Blanca.

B. Local Effects

The ground motion from Rainier was barely felt at 2.5 miles and that from Blanca at 16 miles. There was no structural damage to tunnels or to facilities at or beyond 2500 feet from Blanca. These facilities included a major electronic recording station and a ventilation blower system for the tunnel. These observations give a rough indication of damage radii.

The airblast effects for all shots at scaled depths of 200 $W^{1/3}$ or greater were negligible. These explosions were not audible at a distance of 2.5 miles, although some individuals reported hearing a dull boom from Rainier. While the explosions were not heard by ear, signals were detected by microbarographs in several locations [private communication, Jack W. Reed, Sandia Corp., 1958].

The details of fracturing and bedding plane shifts were mapped and have been described elsewhere [Diment and others 1959]. For Blanca a major section of the top of the mesa shifted down the slope forming a scarp about 70 feet high. The change in profile and area of slumping are shown in Figures 11 and 12 of the Appendix.

C. Earth Motion Measurements

Acceleration and displacement measurements on Rainier by the Stanford Research Institute [Swift and Sachs 1959], Edgerton, Germeshausen and Grier, Inc. [1958] and Sandia Corporation [Perret 1958], indicated that a large earth cap beginning approximately 180 feet below the mesa surface separated from the mesa over the charge and subsequently fell back into place. The only significant vertical displacement occurred at or near surface zero and reached a maximum of 1 foot. The peak acceleration at surface zero was 6 g at 186 milliseconds after zero time.

For Blanca [Swift and others 1959, Morris and Schneiderhan 1959, Perret, to be published] the accelerations measured on the mesa surface show vertical maxima that are consistently larger than the horizontal. The mesa surface directly above the Blanca detonation point was displaced vertically approximately 30 inches in about 400 milliseconds.

Seismic signals from the Rainier event were detected at various stations in the continental U.S. and at distances up to 1000 miles [Diment and others 1959, Carder and others 1958]. Seismic signals were also detected (though barely resolved) at College Station in Fairbanks, Alaska at a distance of 2200 miles.

Seismic effects [Carder and others 1959] resulting from Blanca, Logan, Tamalpais and events of Hardtack Phase-II underground explosions were measured by strong-motion and teleseismic seismographs out to distances of nearly 100 miles. In addition, many temporary seismographs were operated by a number of organizations to distances of nearly 2400 miles, and routine seismographs were operated on a world-wide basis.

Preliminary results indicate that the seismic effects were consistent with empirical formulas developed from Rainier data, except that attenuation of surface waves beyond 200 kilometers may have been higher than the formula for that distance would indicate. Results obtained from the smaller shots require considerably more thought before appraisal. Preliminary seismic data on Logan, for example, indicate that the fraction of energy in the seismic waves is about twice as large as expected from the Rainier formulas.

4. Detailed Local Results

Of the underground explosions, the first one, Rainier, has been studied in most detail and provides most of the data from which a model has been developed. Radioactivity and temperature distributions were determined by drilling and logging a series of holes through the active region. Cores were also recovered and subjected to chemical, radiochemical, and physical property determinations. Similar work, although not in as much detail, has been accomplished for the other explosions. In addition to drilling, two drifts have been driven through the Rainier shot zone. One drift passed about 25 feet below and one about 100 feet above the center of detonation. The layout of drill holes and drifts is shown in Figure 2. Explorations by means of drill holes permitted the determination of the properties of the medium surrounding the center of the explosion.

A. Temperature Distribution

The temperature distribution [Goodale and others 1958, Olsen and others 1959] for Rainier measured five months after detonation is shown in Figure 3.

The energy-content within the various isothermal contours calculated using a mean specific heat of 0.3 cal/g/°C is listed in Table 9.

TABLE 9

Thermal Energy Distribution (Rainier)

Isotherm °C	Average radius feet	Accumulated total energy within isotherm* gram-calories	% of total prompt release
20	100	10^{12}	60
40	80	7×10^{11}	40
60	55	3×10^{11}	17
80	30	6×10^{10}	3

*The temperature distribution was assumed to be axially symmetric.

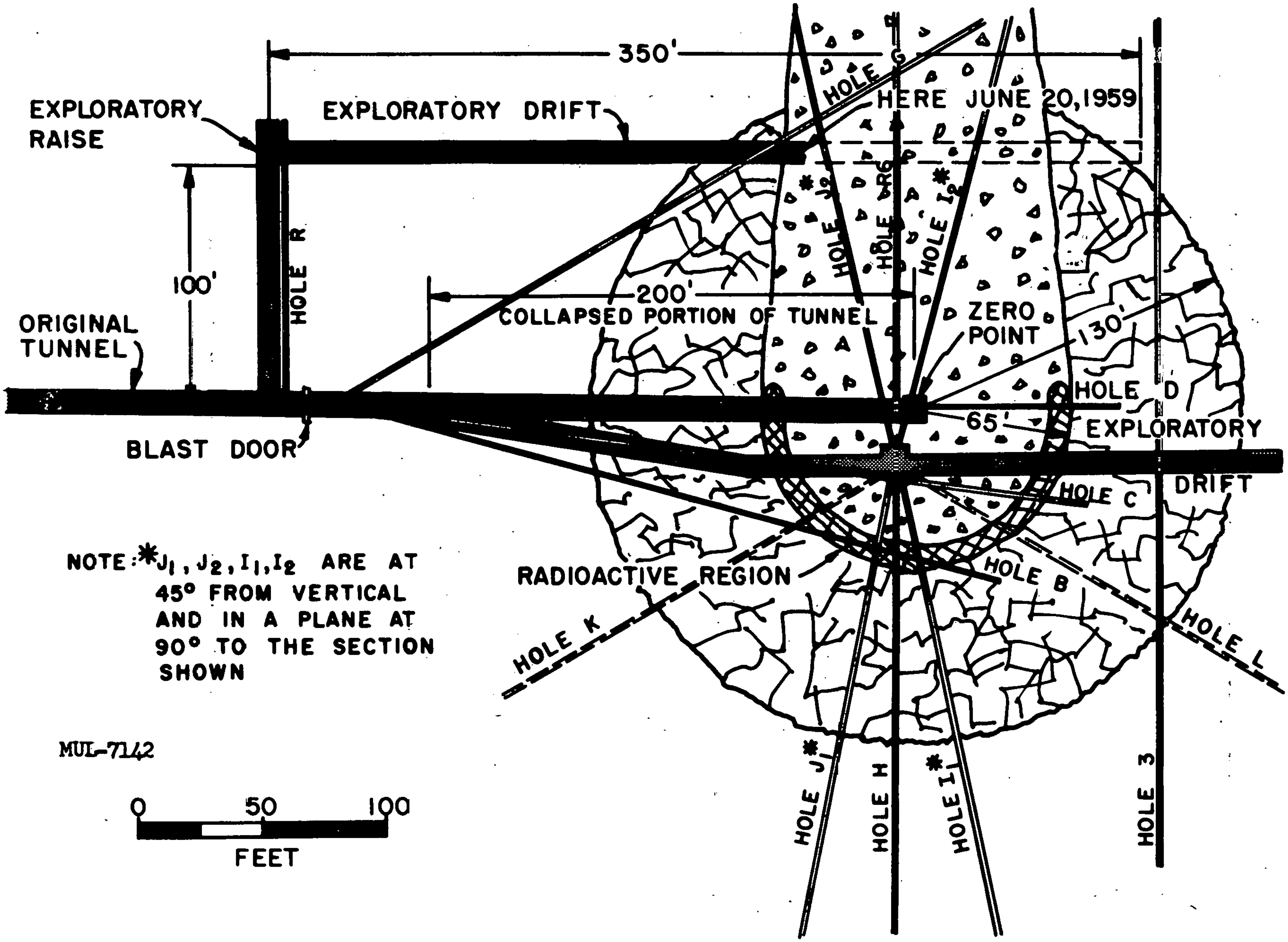

Fig. 2. Drifts and drill holes for post-shot studies of Rainier.

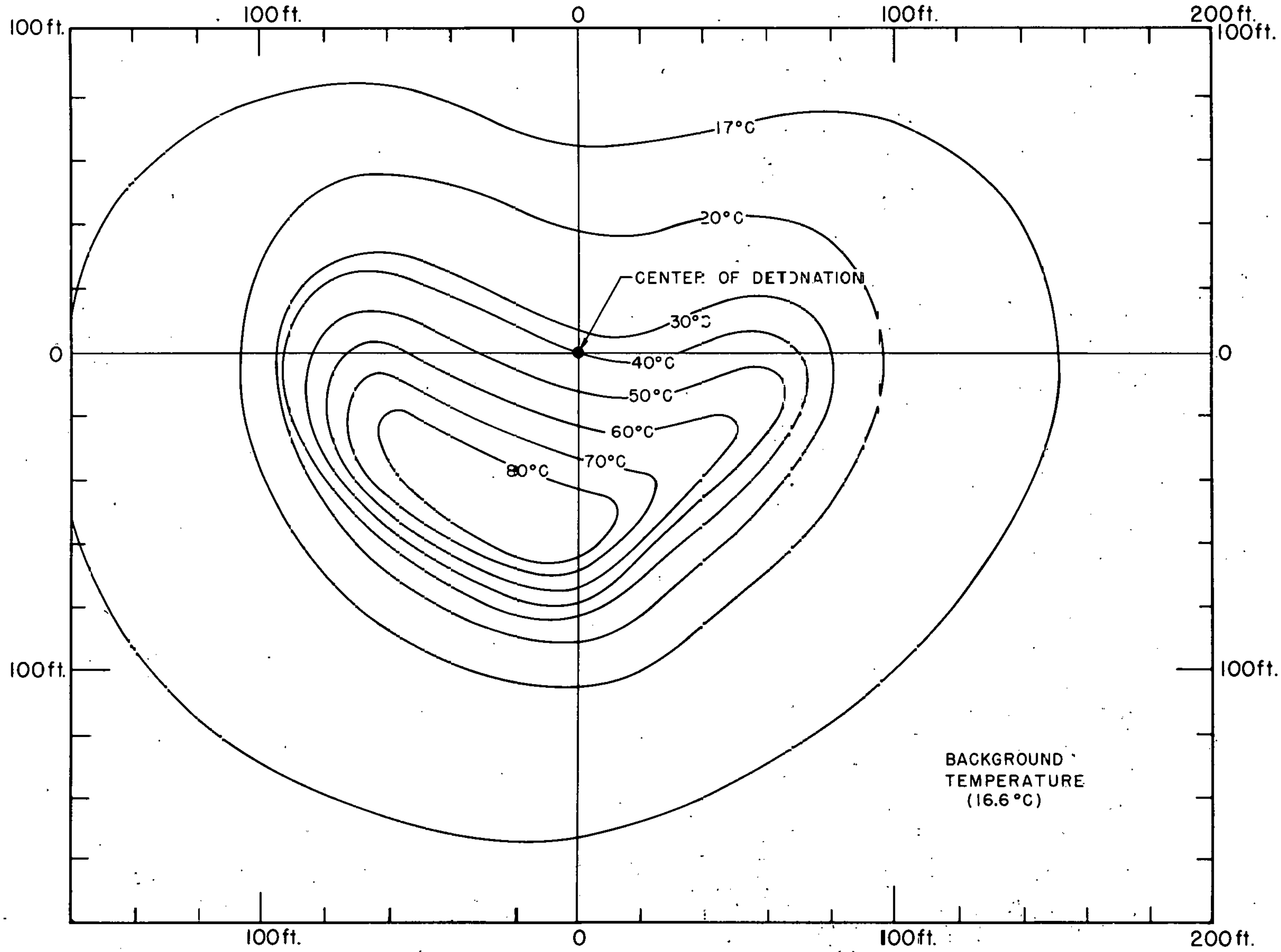

MUL-5941

Fig. 3. Temperature distribution of Rainier, five months after detonation.

The maximum temperature measured within the 80°C contour was 94°C, which is the boiling point of water at the altitude of the explosion.

The temperature distributions for the other explosions have not yet been determined as completely as for Rainier but at least one hole has been logged for each. The general features of the distributions such as the geometry and the maximum temperatures observed were similar to those of Rainier. For Logan and Blanca the minor asymmetry in the temperatures and radiation distributions indicated that there was movement of some of the gases along fissures and in the direction of the tunnels at early times.

For comparative purposes the approximate radii at which various temperatures were observed are listed in Table 10.

TABLE 10

Approximate Average Radii (feet) of Various Isotherms

Isotherm °C	Blanca	Logan	Rainier	Tamalpais
20	(240)*	(190)*	100	---
40	120	100	80	---
60	---	80	55	---
80	---	70	30	---
R_T (feet)	210	140	96	50
$\frac{R_T}{W^{1/3}}$ (ft/kt$^{1/3}$)	79	82	81	121**

(R_T is the radius at which temperature first rises sharply.)

*(The background temperatures for Blanca and Logan were 20°C and 18°C, respectively.)

**Fired in a large room.

From these data R_T can be scaled according to the expression: $R_T = 81\ W^{1/3}$. The center of the Rainier temperature distribution appears to be displaced laterally about 20 ft. It is possible that the early gas venting took place in such a direction as to account for this effect. A large open vertical fault did exist 50 feet from that side of the point of detonation, but whether venting actually occurred into this region is not known.

B. Distribution of Radioactivity

The general distribution of radioactivity was determined by logging drill holes through the active region and by surveying the areas of fallout for those explosions that released activity to the atmosphere. The gross distribution [Olsen and others 1959] as measured by thick-walled ion chambers for Rainier is shown in Figure 4. It is noted that the activity is concentrated in a bowl-like shell several feet thick. This same general distribution was noted from the other explosions. The mean radii of the radioactive zones are listed in Table 11 [Olsen and others 1959]. A scaling law $R = 50\ W^{1/3}$ feet is derived from the scaled radii of the radioactive shells produced by the three large explosions.

TABLE 11

Radii of Radioactive Shells

Event	Radius (feet)	Scaled radius ($R/W^{1/3}$ feet/kt$^{1/3}$)
Neptune	21	47*
Blanca	130	48
Logan	85	50
Rainier	62	52
Tamalpais	30	73**

*Cratering shot

**Fired in a large room

It was determined that the bulk of the radioactivity was concentrated in glass formed by the explosion. From the radiochemical analysis of this material it was concluded that 500±150 tons of rock were melted per kiloton of energy release. The glass contained between 60% and 85% of the gross fission products. However, those materials with gaseous precursors were depleted in the glass by as much as a factor of 100 from the nonvolatile species. These volatile isotopes were correspondingly enriched outside the radioactive shells.

Since the fission products are comprised of many elements their volatilities range from very large (krypton, xenon) to very small (zirconium, cerium). The relative abundance of those species which are gaseous and refractory changes as radioactive decay processes proceed after the detonation.

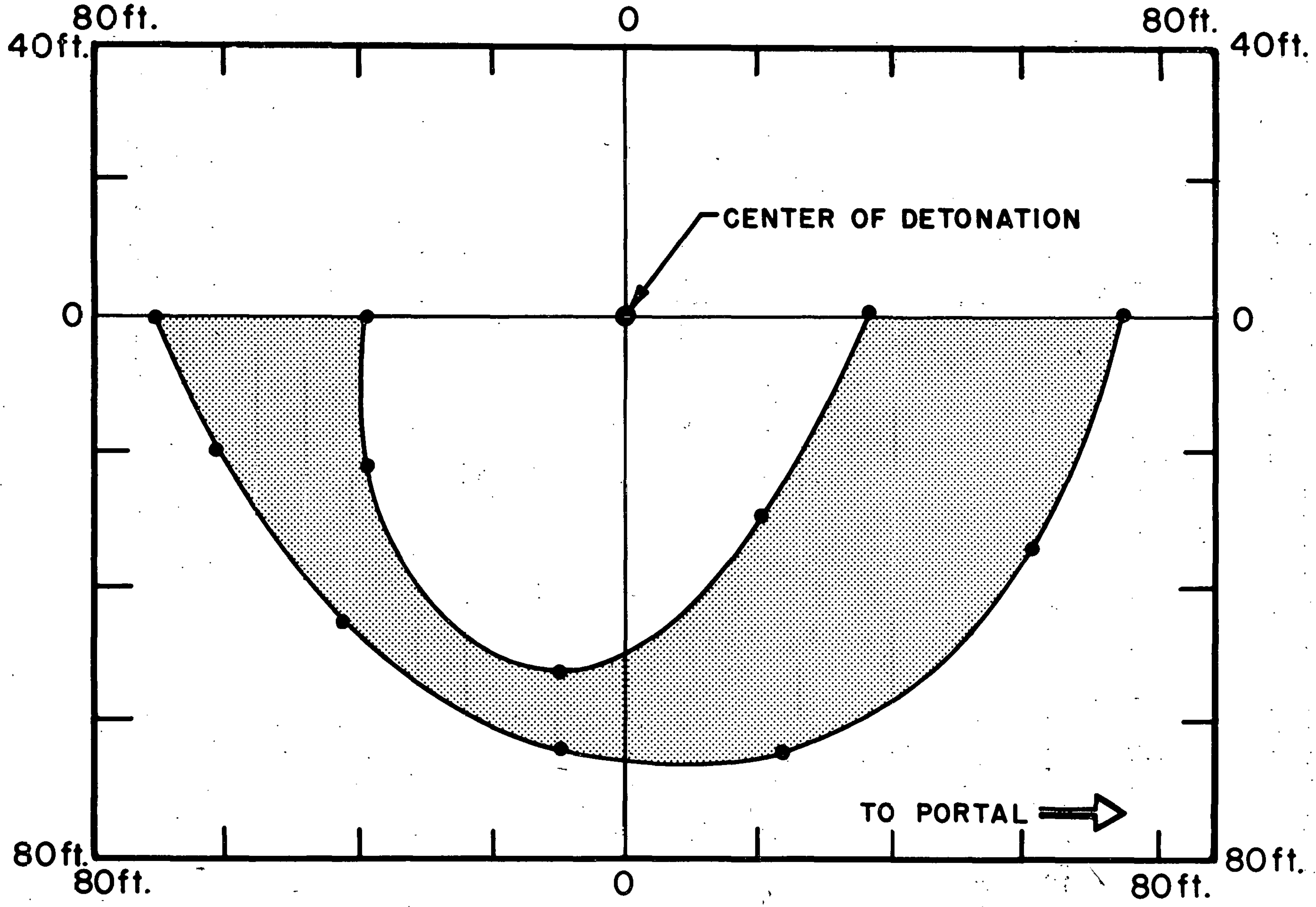

MUL-7161

Fig. 4. Distribution of radioactivity — Rainier Event.

Table 12 is a list of the parent-daughter relationships leading to some of the isotopes which were later determined radiochemically.

TABLE 12

Decay Chains Leading to Isotopes Which Have Been Measured in Debris from Underground Explosions

Mass	Element, half-life and measured isotope (underlined)								
85	As	$\xrightarrow[\text{sec}]{0.43}$	Se	$\xrightarrow[\text{sec}]{40}$	Br	$\xrightarrow[\text{min}]{30}$	$\underline{\text{Kr}}$		
89	Kr	$\xrightarrow[\text{min}]{3.2}$	Rb	$\xrightarrow[\text{min}]{1.5}$	$\underline{\text{Sr}}$				
90	Kr	$\xrightarrow[\text{sec}]{33}$	Rb	$\xrightarrow[\text{min}]{2.7}$	$\underline{\text{Sr}}$				
91	Kr	$\xrightarrow[\text{sec}]{9.8}$	Rb	$\xrightarrow[\text{min}]{2}$	Sr	$\xrightarrow[\text{hour}]{9.7}$	$\underline{\text{Y}}$		
95	Rb	$\xrightarrow{\text{sh}}$	Sr	$\xrightarrow{\text{sh}}$	Y	$\xrightarrow[\text{min}]{10}$	$\underline{\text{Zr}}$		
99	Zr	$\xrightarrow[\text{sec}]{30}$	Nb	$\xrightarrow[\text{min}]{2.5}$	$\underline{\text{Mo}}$				
137	I	$\xrightarrow[\text{sec}]{22}$	Xe	$\xrightarrow[\text{min}]{3.8}$	$\underline{\text{Cs}}$				
140	Xe	$\xrightarrow[\text{sec}]{16}$	Cs	$\xrightarrow[\text{sec}]{66}$	$\underline{\text{Ba}}$				
141	Xe	$\xrightarrow[\text{sec}]{1.7}$	Cs	$\xrightarrow{\text{sh}^{a}}$	Ba	$\xrightarrow[\text{min}]{18}$	La	$\xrightarrow[\text{hour}]{3.7}$	$\underline{\text{Ce}}$
144	Cs	$\xrightarrow{\text{sh}^{a}}$	Ba	$\xrightarrow{\text{sh}^{a}}$	La	$\xrightarrow{\text{sh}}$	$\underline{\text{Ce}}$		

[a] sh — short (compared to a few seconds.)

The effect of the gaseous ancestors in leading to the depletion of certain nuclides from the glass and their enrichment in the vented material is demonstrated in Table 13. These data are the summarized radiochemical results from all of the explosions in tuff.

TABLE 13

Summary of Radiochemical Data from Several Underground Explosions

Isotopes*	Percentage of total in fused material	Degree of enrichment in rubble chimney	Degree of enrichment in vented material***
Kr^{85}	< 1%	~ 0	All in gas
Sr^{89}, As	3 - 10%	> 2	~ 10
Sr^{90}, Cs^{137}	20 - 40%	> 2	~ 5
Y^{91}, Ba^{140}, Ce^{141}, Cs	30 - 60%	> 2	> 2
U, Mo^{99}	50 - 100%	< 2	< 2
Pu, A.E.**, Pa, Hf			
Ta, Ce^{144}, Nd^{147}	~ 100%	1.0	1.0

*Examples which have been measured.
**A.E. represents actinide earth.
***Observed from Neptune and Blanca.

It should be noted that since Sr^{89} and Sr^{90} are strongly depleted in the glass debris, the gases must have escaped from the glass in times comparable to the half-lives of their krypton ancestors (3.2 minutes and 33 seconds). At the temperatures in the cavity, around 1000° or 1500°C, several other fission products are volatile and also appear to be depleted from the glass and enriched in the vented material. Arsenic, cesium, and uranium appear to behave in this way.

5. Phenomenology

The following discussion largely pertains to Rainier since most of the measurements have been completed at that site. Based on the fact that the radioactivity and temperature distributions were concentrated in shells and that within these shells the region was generally permeable to drill water, while outside it was much less permeable, led to the conclusion that the explosions produced cavities of radius $R = 50\ W^{1/3}$ feet, which stood for a short time, then collapsed.

In the case of Rainier, the description of the state of the cavity at this time and its collapse has been described by Kennedy and Higgins [1958]. The cavity when first formed was lined with about 4 inches of melted rock and filled with steam at a pressure of 40 atmospheres, which is approximately the lithostatic pressure. The cavity stood long enough, between 30 seconds and 2 minutes, for much of the fluid rock to flow down the sides and to drip from the roof. At this time the cavity began to collapse and cooled rapidly due to expansion of the steam. The sudden cooling quenched some of the droplets of rock in free fall, as well as some of the 'icicles' as they hung suspended from the cavity roof. The cavity was filled with broken rock from the collapse, and the caving progressed vertically to a distance of 386 feet above the point of detonation.

Inspection of the interior of the collapsed zone revealed the distribution of size of blocks formed. The blocks in the lower drift varied from a few inches in diameter, just inside the radioactive zone, up to several feet in diameter near the center. The regions between the blocks were filled with pulverized material which had resolidified by the time the re-entry was accomplished one year after the explosion. The recementing is not surprising for material with high clay content.

The drift, 100 feet above the zero point, first broke into a block-caved region 75 feet out from the vertical line passing through the center of detonation. At this point the blocks were a few inches to a few feet in diameter with open fractures, then graduated down to a fine powder at a distance of 65 feet. At a distance of 40 feet a large cavity was encountered. In summary the collapse of the initial cavity produced a broken permeable zone that appears to be cylindrical with a radius of 65-75 feet for the first 100 feet of height, and with a total height of about 386 feet. The radius of the collapsed zone above 100 feet has not yet been measured.

Soon after detonation the high temperature rocks rapidly cooled to the boiling point of water (94°C, at this altitude - 6600 feet), because of the water content of this tuff and the large permeable zone resulting from the collapse of the cavity. The diffusion of heat then took place at a lower rate leading to the observed distribution measured five months after detonation (Figure 3).

The Rainier device was detonated in a room 6'×6'×7', which contained about one ton of material. The initial temperature and pressure in the room can be calculated as follows:

$$\text{Energy density:}\quad E = E_p + E_r = \frac{3}{2}\, n\, kt + \frac{4\sigma T^4}{c}$$

where
E_p = energy density in the particles
E_r = energy density in radiation
n = $A_o\rho/M$ = number of particles per cm^3
k = 1.37×10^{-16} erg/°K (Boltzmann's constant)
T = Temperature °K
σ = 5.74×10^{-5} erg/cm^2/°K^4 (Stefan-Boltzmann constant)
c = 3×10^{10} cm/sec (velocity of light)
A_o = 6.04×10^{23} (Avogadro's number)
M = molecular weight
ρ = density in g/cm^3

This can be put in the form

$$E = 3/2\ \frac{A_o\rho}{M}\ k\,T + \frac{4\sigma T^4}{c}$$

$$= 1.25\times10^8\ \frac{\rho}{M}\ T + 7.65\times10^{-15}\ T^4 \quad \text{erg/cm}^3$$

The pressure equals 2/3 particle energy density plus 1/3 radiation energy density thus

$$P = 0.83\times10^8\ \frac{\rho}{M}\ T + 2.55\times10^{-15}\ T^4 \quad \text{dynes/cm}^2$$

The prompt energy release of the Rainier explosion was 7.2×10^{19} ergs. Since the mass of material in the room was about 10^6 g and the volume was 7×10^6 cm^3, the mean density was 0.14 g/cm^3. At extremely high temperatures essentially all electrons are stripped from nuclei and since the atomic weight is approximately twice the atomic number, the effective molecular weight is given by

$$M_{eff} = \frac{\Sigma N_i \times 2 Z_i}{\Sigma N_i (Z_i + 1)} \approx 2$$

where N_i is the number of atoms of atomic number Z_i and the summation is taken over all atoms in the zero room. Applying these numbers as indicated leads to the fact that the temperature a few microseconds after detonation was about 1,000,000°K and the pressure 7,000,000 atmospheres (bars). The radiation pressure at this temperature is 2500 bars.

The calculation of the behavior of the medium from this point onward was carried out by J. Nuckolls [1959], who extended the earlier calculations of Pelsor [private communication]. Nuckolls' treatment involved the development of a code for a computer calculation of the behavior of the medium from a few microseconds to about 100 milliseconds. This time was sufficiently long to permit calculation of all the dynamic behavior of the system. Only the general results of this calculation will be given here.

It was assumed that tuff has negligible large-scale tensile strength and behaves as a linear elastic solid as long as the tension does not exceed the stress due to overburden pressure. The elastic constants used in the calculation were the measured values for bulk modulus, shear modulus, and sound speed. After the tension in the spherical shell exceeds the lithostatic stress the components of the stress tensor are set equal to a pressure (shear modulus equal to zero) which is related to the volume by a bulk modulus type equation of state.

From the calculations, the shock time-of-arrival was determined. This information together with the measured results of Porzel [Cohn and others, to be published] are shown in Figure 5. In Figure 6 the peak shock pressure as a function of radius is given. It decreases as $r^{-2.35}$ out to about ten meters. The tuff was vaporized to a radius of 2.3 meters in 0.2 milliseconds (peak pressure 1.0 megabar) and melted by shock to 3.3 meters (0.4 mb). Enough energy was deposited by the shock in the first 4.6 meters to melt all the tuff within this radius (660 tons). Radiochemical analysis on Rainier gave about 800 tons. This total amount melted is the sum of the shock induced melting (660 calculated) and the melting induced by fission-product decay energy and should be about 1.2 times larger than the shock induced melting alone. The factor 1.2 results from the ratio of the percentage of prompt energy in gas + liquid + fission product divided by the prompt energy in gas + liquid.

The shock progressed outward and crushed the medium to a radius of 130 feet where the pressure was 1.4 kilobars, or twice the static compressive strength. The elastic radius was calculated to be 285 feet horizontally and 305 feet vertically.

It was calculated that a spherical cavity was formed which expanded outward as the shock advanced. The melted tuff formed the inner surface of this cavity. The calculated rate of growth of the cavity is given in Figure 7. It is noted that it reached its maximum radius of 62 feet in about 80 milliseconds. The radius that was determined experimentally is in agreement with this value.

Nuckolls also calculated the energy and temperature distribution at 90 milliseconds after detonation. At this time, less than 0.5 percent of the energy is kinetic energy and therefore the system is essentially static (Table 14).

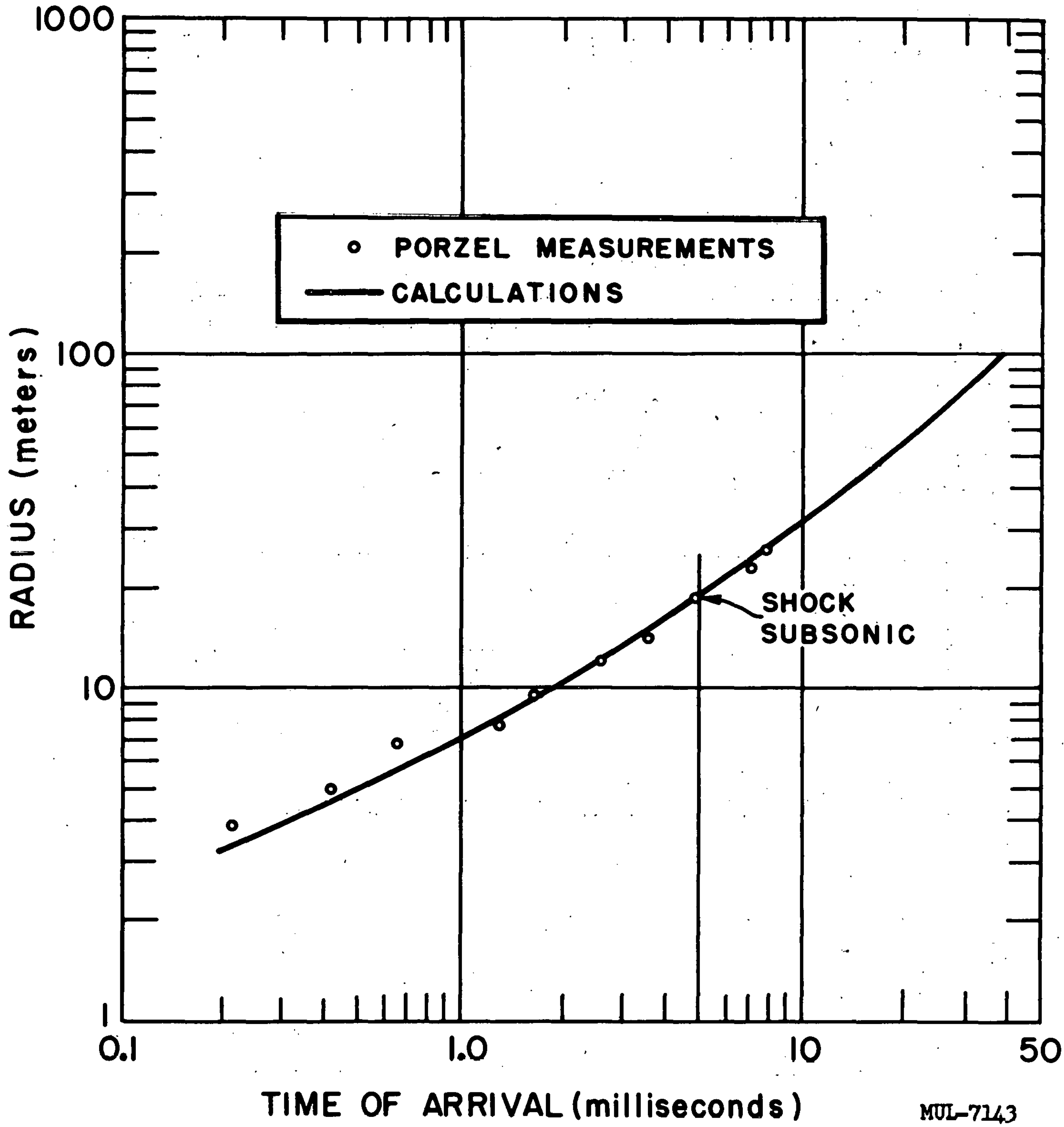

Fig. 5. Shock time-of-arrival — Rainier Event.

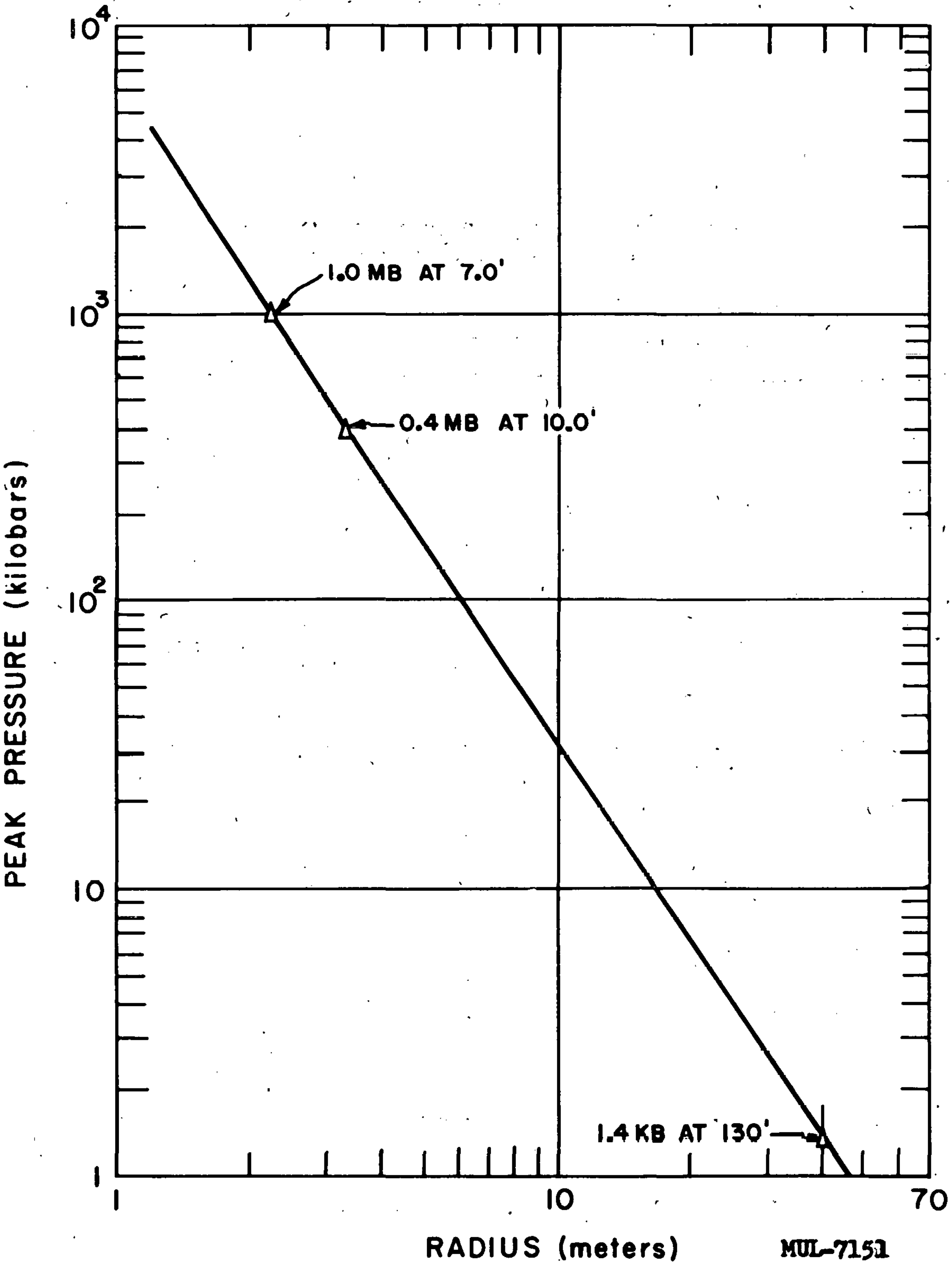

Fig. 6. Peak shock pressure – Rainier Event.

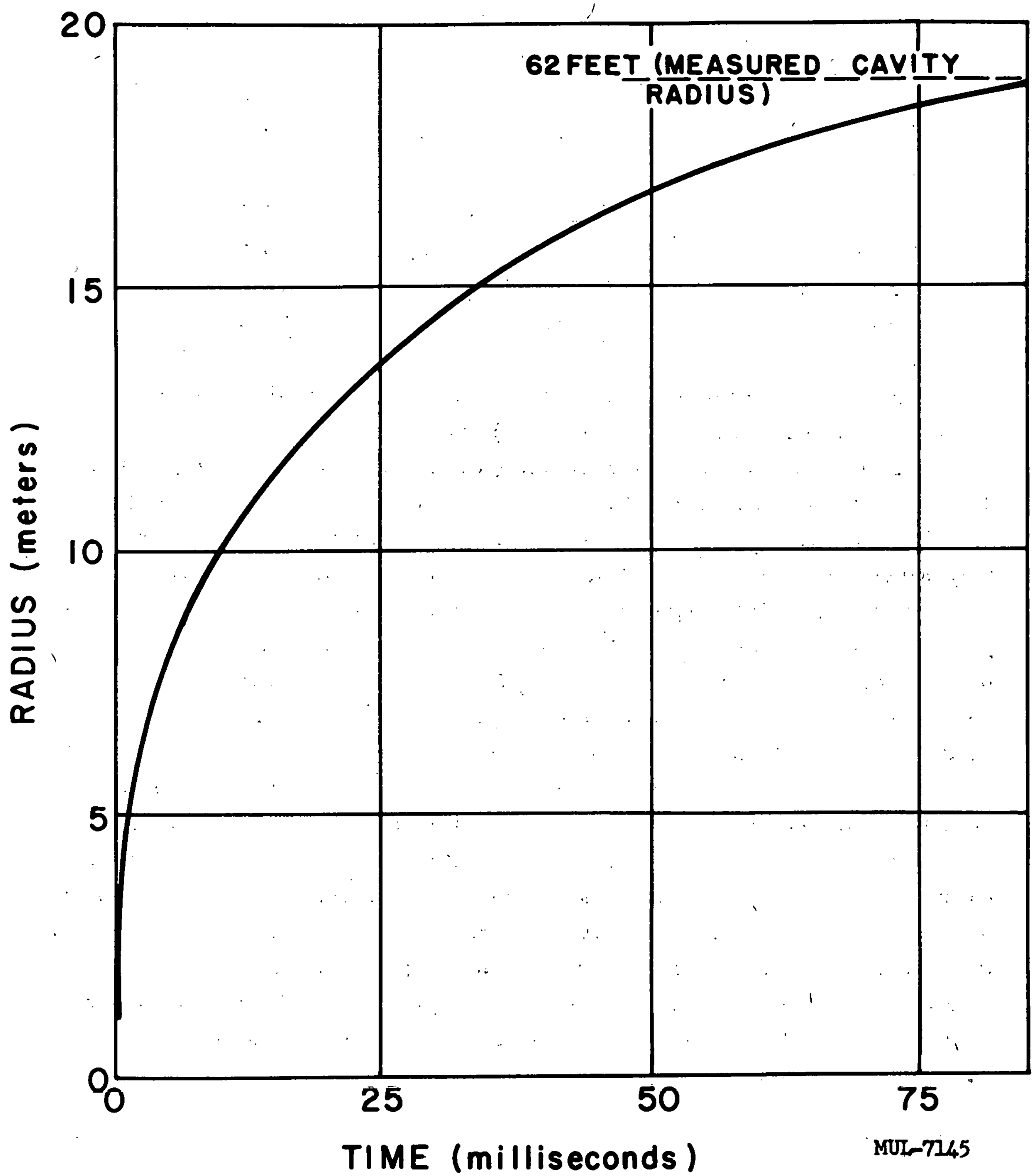

Fig. 7. Rate of growth of Rainier cavity.

TABLE 14

Rainier Energy Distribution

State	Radii	Percentage of prompt energy
Gas	0 - 62 ft	8.2
Liquid	62 ft - 62-1/4 ft	19.1
Crushed	62-1/4 ft - 130 ft	47.0
Fractured	130 ft - 280 ft	21.2
Elastic	280 ft	4.5

The calculated temperature distribution after the cavity had ceased to grow but before it collapsed is shown in Figure 8.

From the known melting properties of tuff, it was concluded [Nuckolls 1959] that the melted material at this time must have been at a temperature of 1200-1500°C. To heat 800 tons of tuff (15 percent water) to this temperature range would require about 5.7×10^{11} calories. This is 32 percent of the total energy release (prompt plus fission product heat) of the Rainier explosion (1.8×10^{12} calories). Nuckolls' calculation gives 27 percent of the prompt release (1.70×10^{12} calories). Since the energy of fission-product decay should contribute between 3 and 4 percent additional to the prompt melting energy, the numbers are consistent.

By assuming that all of the water from the molten and vaporized rock remains in the cavity as steam and that the temperature is about the same as the molten rock (1500°C), the pressure due to steam in the cavity can be calculated to be 40 bars, which can be compared with the lithostatic pressure of 50 to 55 bars. An experimental confirmation [Kennedy and Higgins 1958] of this estimate was made by heating some of the glass, which had condensed in free fall in a vacuum furnace to drive out the gas. From the measured quantity of trapped gas, it was found that the pressure in the contained bubbles was 40 bars, which agrees with the calculated value.

6. Summary

1. The radioactivity of nuclear explosions in the kiloton range in tuff can be completely contained underground at depths of $D = 400\ W^{1/3}$ feet or greater.

2. The initial cavity formed by the explosion has a radius of $R = 50\ W^{1/3}$ feet.

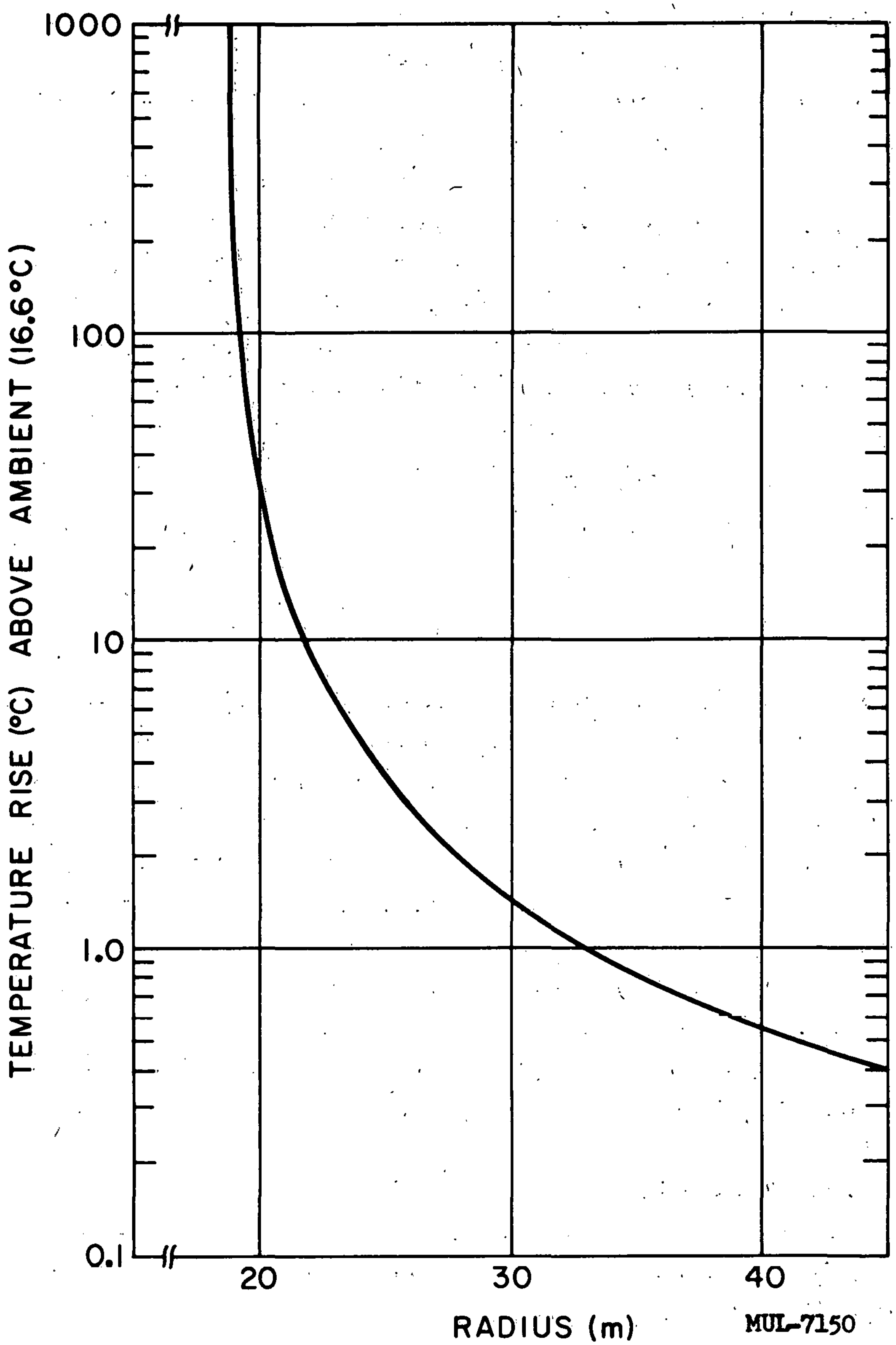

Fig. 8. Initial Rainier temperature distribution.

3. Initially melted rock, which is converted to glass on cooling, amounts to 500 ± 150 tons per kiloton of energy release.

4. The collapse of the cavity produces a zone of about 70,000 yds^3/kt (120,000 tons/kt) of broken permeable material.

5. The major portion (65-80 percent) of the gross fission product activity is in dilute (one part per 10,000,000) solution in glass. The remainder (20-35 percent) is distributed throughout the collapsed zone of the chimney and is deposited on the surface of the broken material.

6. About 30 percent of the total energy release of the explosion is initially deposited in steam and hot rock at a temperature in excess of 1200°C. This temperature rapidly degrades to the boiling point of water. One year after the Rainier explosion this energy resided within a volume whose radius was less than 80 feet.

References

Carder, D.S., Cloud, W.K., Murphy, L.M. and Hershberger, J.H., 1958. Surface motions from an underground explosion. WT-1530.

Carder, D.S., Cloud, W.K., Pearce, T.H. and Murphy, L.M., 1959. Surface motions from a series of underground nuclear tests. ITR-1705.

Cohn, S., Hoehn, A., Dickens, R.G., Porzel, F.B., Shiffman, T., Hoenig, S., Wilde, N. and Greenberg, C., to be published. Close-in time-of-arrival measurements for yield of UG shot. WT-1495.

Diment, W.H., Wilcox, R.E., Keller, G.V., Dobrovolny, E., Kracek, F.C., Roller, J.C., Peselnick, L.C., Robertson, E.C., Lachenbruch, A.H. and Bunker, C.M., 1958a. Properties of Oak Springs formation in Area 12 at the Nevada Test Site. U.S. Geological Survey, Trace Elements Report 672.

Diment, W.H., Wilmarth, V.R., Houser, F.N., McKeown, F.A., Hinrichs, E.H., Botinelly, T., Wilcox, R.E., Clebsch, A. Jr., Winograd, I.J., Hawley, C.C. and Manger, G.E., 1958b. U.S. Geological Survey, Trace Elements Report 728.

(continued)

References (continued)

Diment, W.H., Wilmarth, V.R., Wilcox, R.E., Clebsch, A. Jr., Manger, G.E., Hawley, C.C., Keller, G.V., Robertson, E.C., Peselnick, L.C., Bunker, C.M., Healey, D.L., Kane, M.F., Roth, E.F., Stewart, S.W., Roller, J.C., Jackson, W.H., Oliver, H.W., Byerly, P.E. and Mabey, D.R., 1959. Geologic effects of the Rainier underground nuclear explosion. U.S. Geological Survey, Trace Elements Report 355.

Edgerton, Germeshausen and Grier, Inc., staff of, 1958. Photographic analysis of earth motion, shot Rainier. WT-1532.

Goodale, T.C., Ragent, B., Samuel, A.H., Anderson, A.L., Nielsen, D.E., and Olsen, J.L., 1958. Temperatures from underground detonation, shot Rainier. WT-1527.

Griggs, D. and Teller, E., 1956. Deep underground test shots. Lawrence Radiation Laboratory, University of California, UCRL-4659.

Johnson, G.W., Pelsor, G.T., Preston, R.G. and Violet, C.E., 1958. The underground nuclear detonation of Sept. 19, 1957, Rainier. Lawrence Radiation Laboratory, University of California, UCRL-5124.

Johnson, G.W. and Violet, C.E., 1958. Phenomenology of contained nuclear explosions. UCRL-5124, Rev. 1. (Available from the Office of Technical Services, Dept. of Commerce, Washington 25, D.C.)

Kennedy, G.C. and Higgins, G.H., 1958. Temperatures and pressures associated with the cavity produced by the Rainier Event. UCRL-5281. (Available from the Office of Technical Services, Dept. of Commerce, Washington 25, D.C.)

Morris, R.H. and Schneiderhan, R.C., 1959. Earth motion studies. ITR-1706.

Nuckolls, J., 1959. Computer calculation of Rainier. Paper presented at Plowshare Symposium, San Francisco, California, May 13, 14, and 15, 1959 (to be published).

Olsen, J.L., Bennet, W.P. and Nielsen, D.E., 1959. Paper presented at Plowshare Symposium, San Francisco, California, May 13, 14, and 15, 1959 (to be published).

Perret, W.R., 1958. Subsurface motion from a confined underground detonation — Part I. Sandia Corporation. ITR-1529.

(continued)

References (continued)

Swift, L. M., Sachs, D.C. and Wells, W. M., 1959. Earth motion measurements. Part I. Seismic studies and cavity studies. ITR-1702.

Swift, L. M. and Sachs, D. C., 1959. Surface motion from an underground detonation. WT-1528.

Warner, S.E. and Violet, C.E., 1959. Properties of the environment of underground nuclear detonations at the Nevada Test Site. UCRL-5542. (Available from the Office of Technical Services, Dept. of Commerce, Washington 25, D.C.)

Note: ITR and WT reports are available from the Office of Technical Services, Dept. of Commerce, Washington 25, D.C.

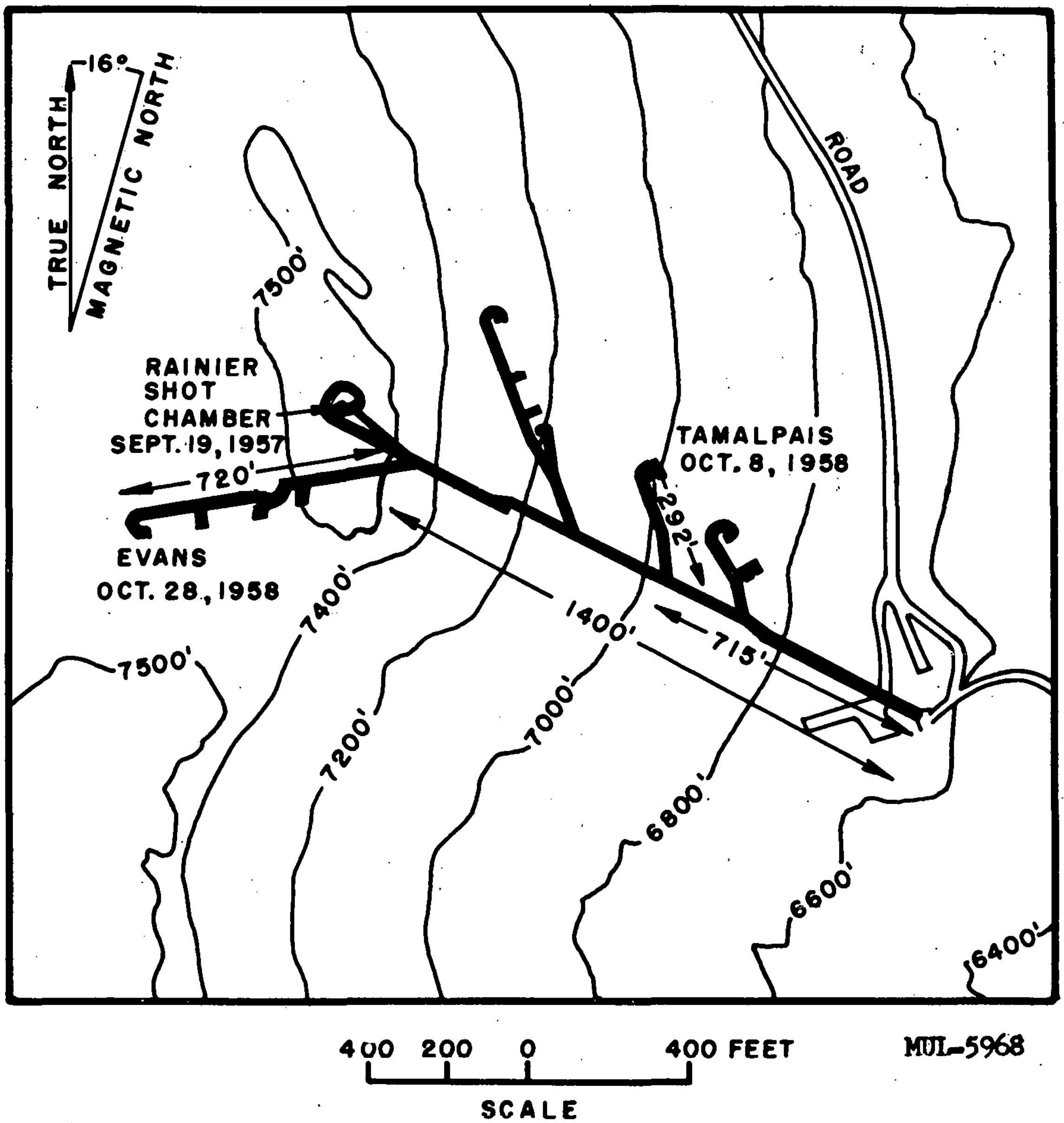

Fig. 1, Appendix. Plan view of Rainier, Evans and Tamalpais sites.

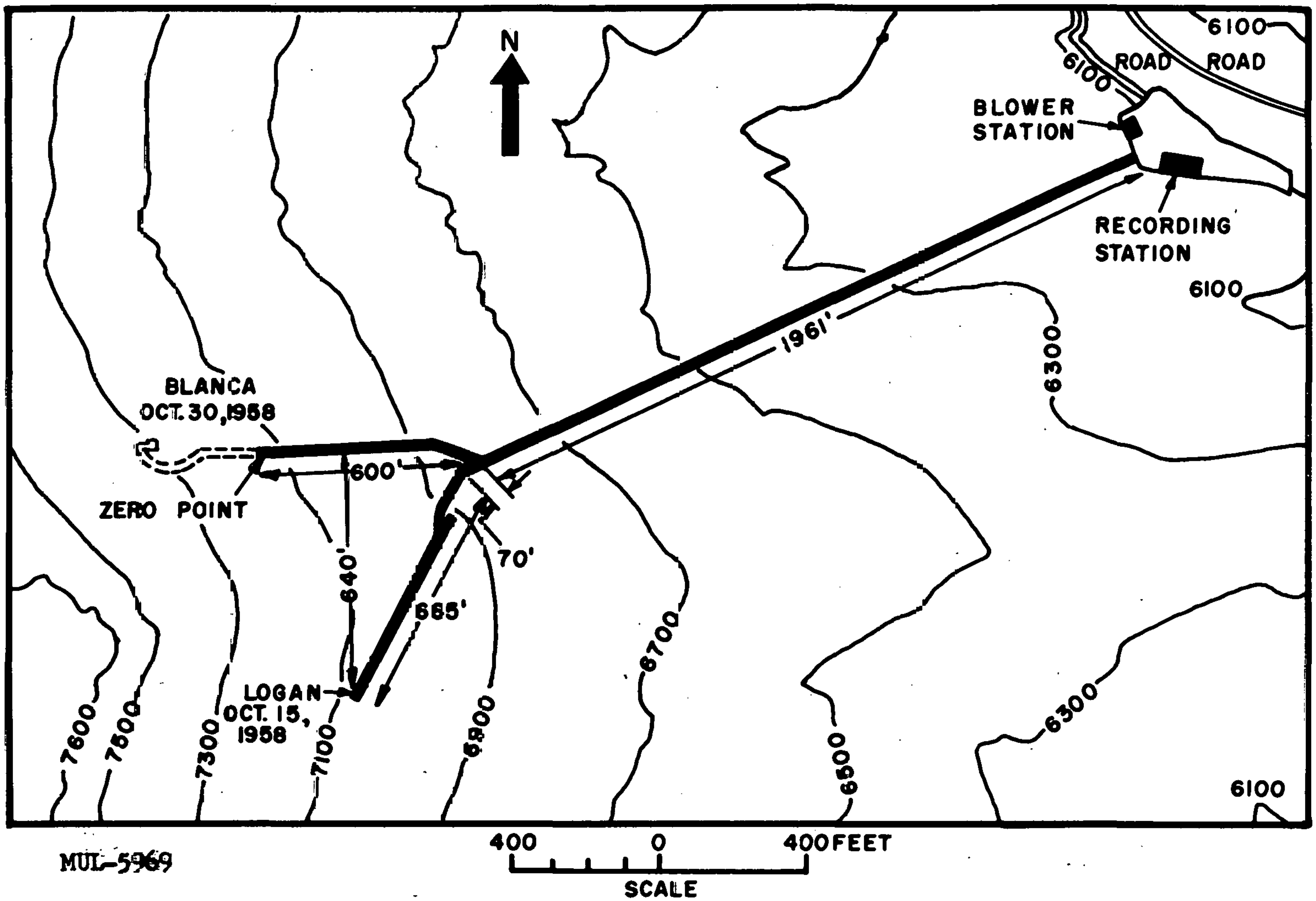

MUL-5969

MAP SHOWING LOCATION OF U12e TUNNEL, RAINIER MESA, NYE COUNTY, NEVADA

Fig. 2, Appendix. Plan view of Blanca and Logan sites.

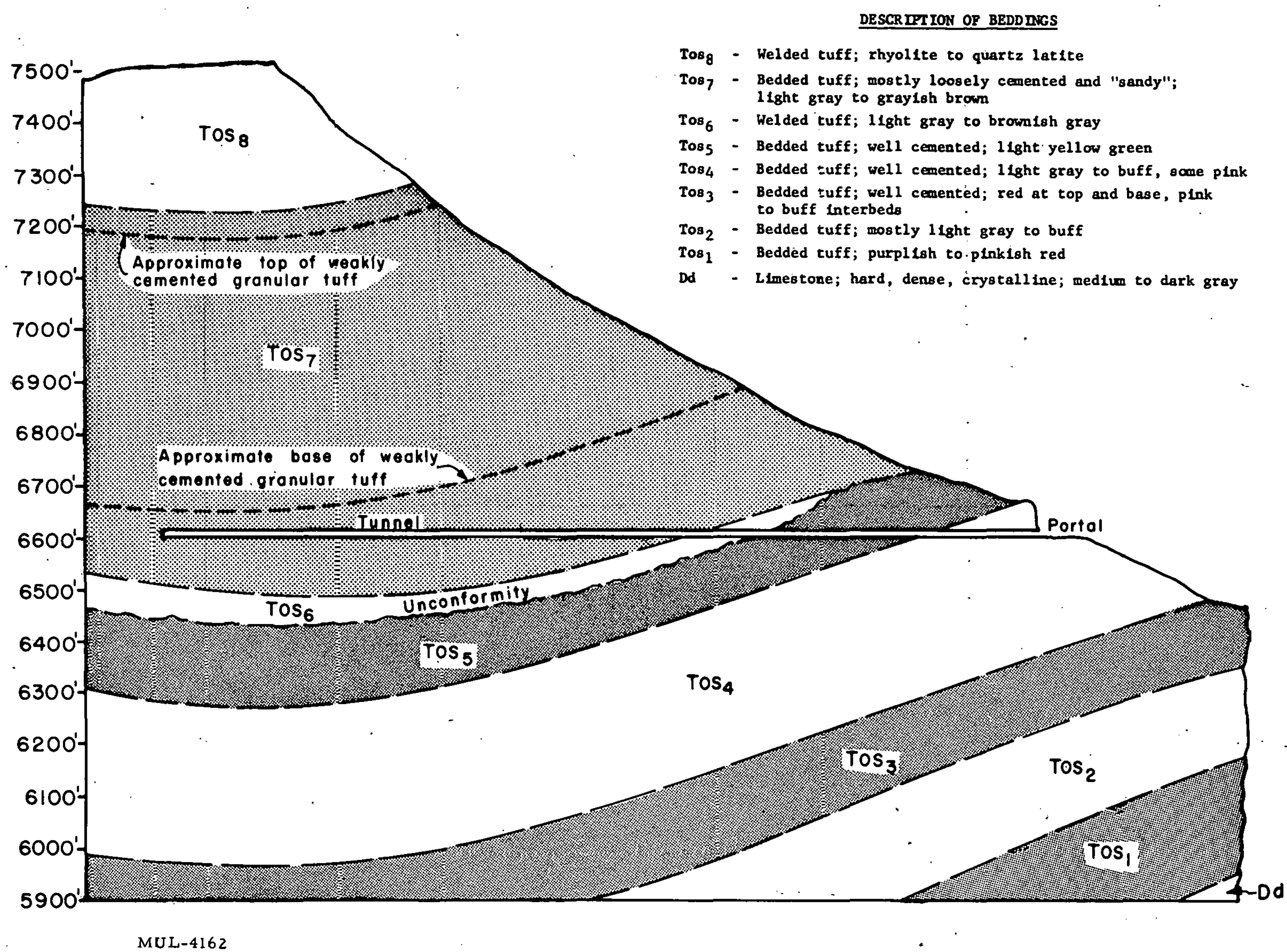

Fig. 3, Appendix. Profile of Rainier site.

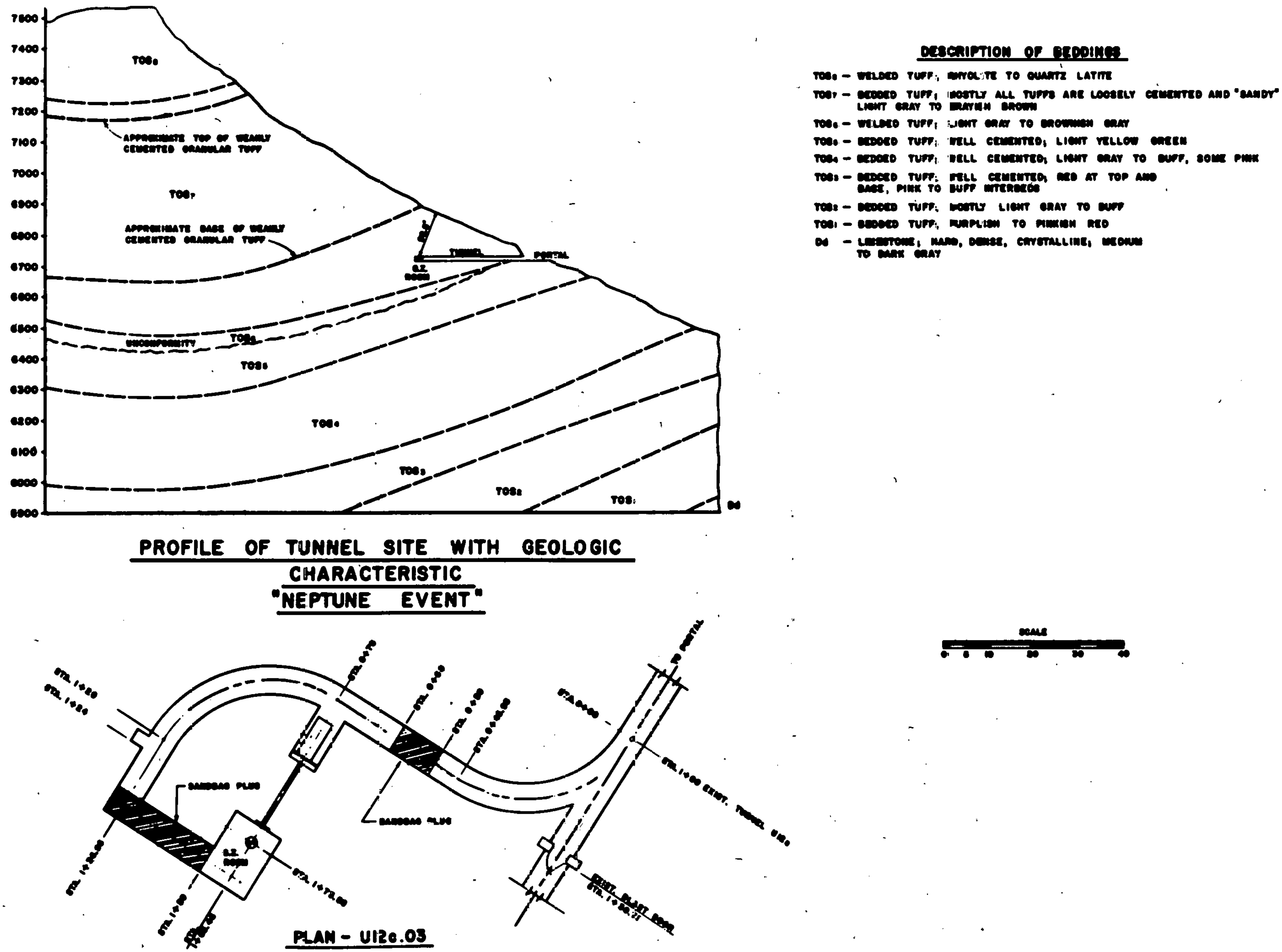

MUL-7167

Fig. 4, Appendix. Plan of Neptune tunnel.

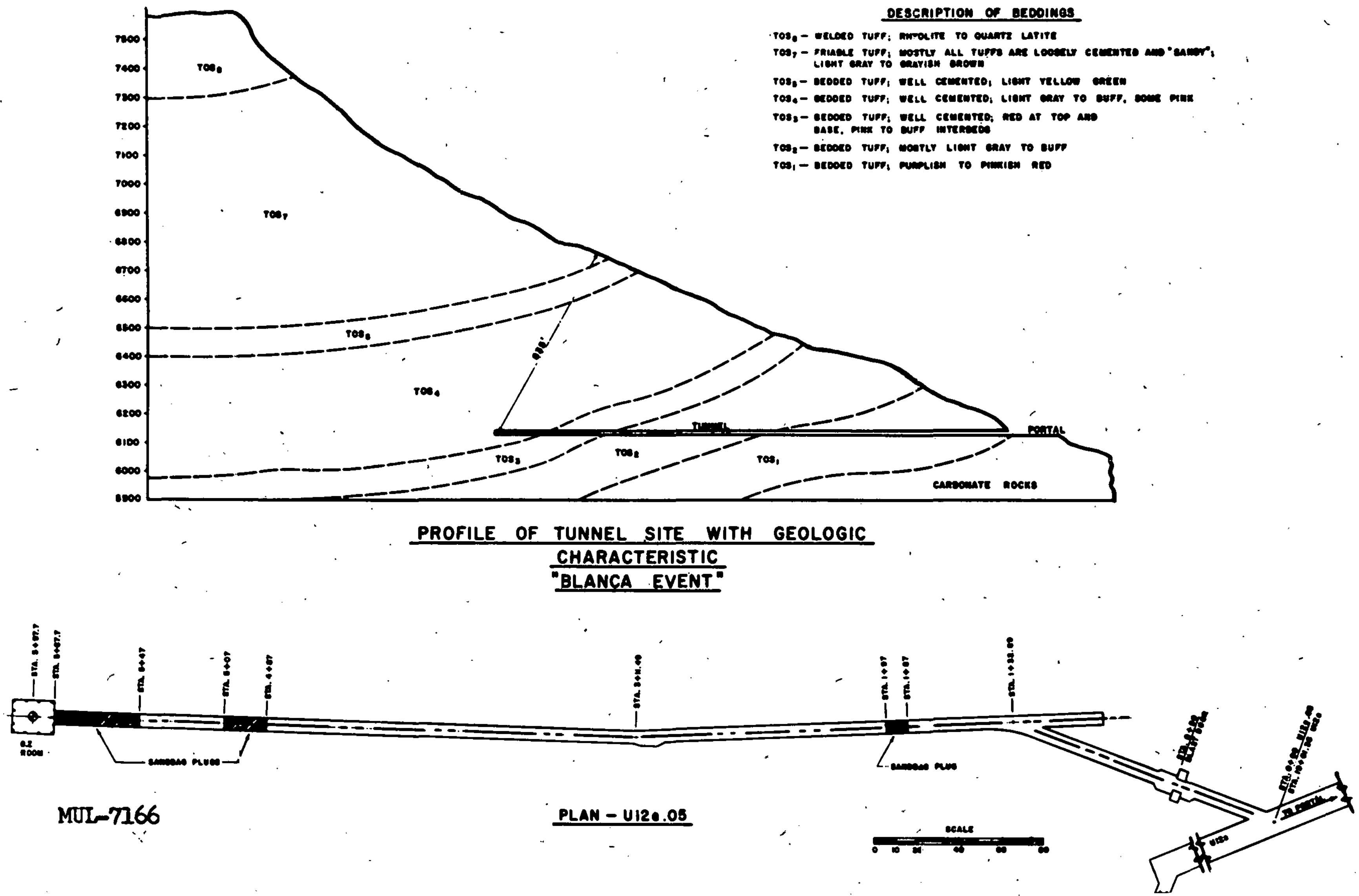

Fig. 5, Appendix. Profile of Blanca site.

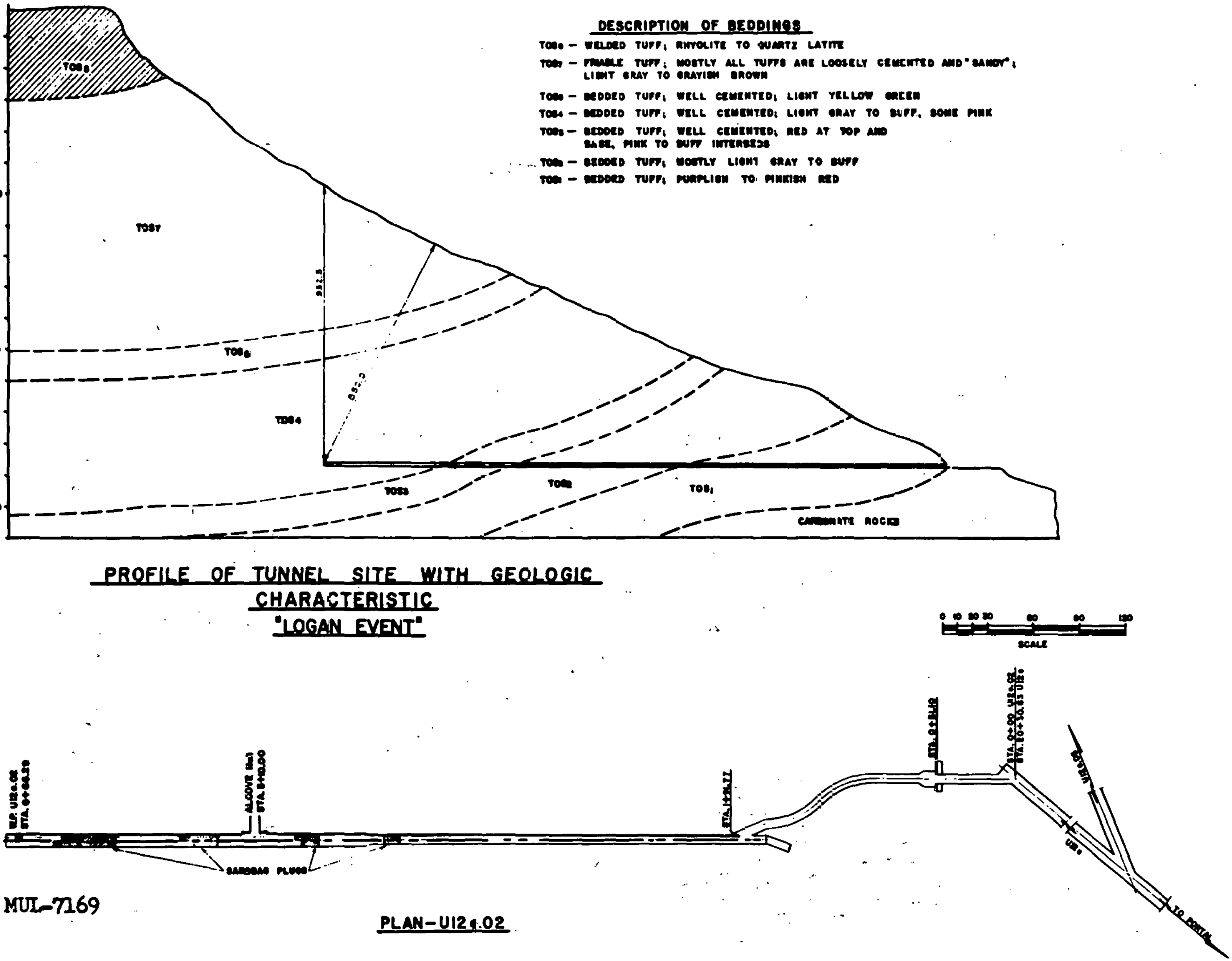

MUL-7169

Fig. 6, Appendix. Profile of Logan site.

- 37 -

UCRL-5626

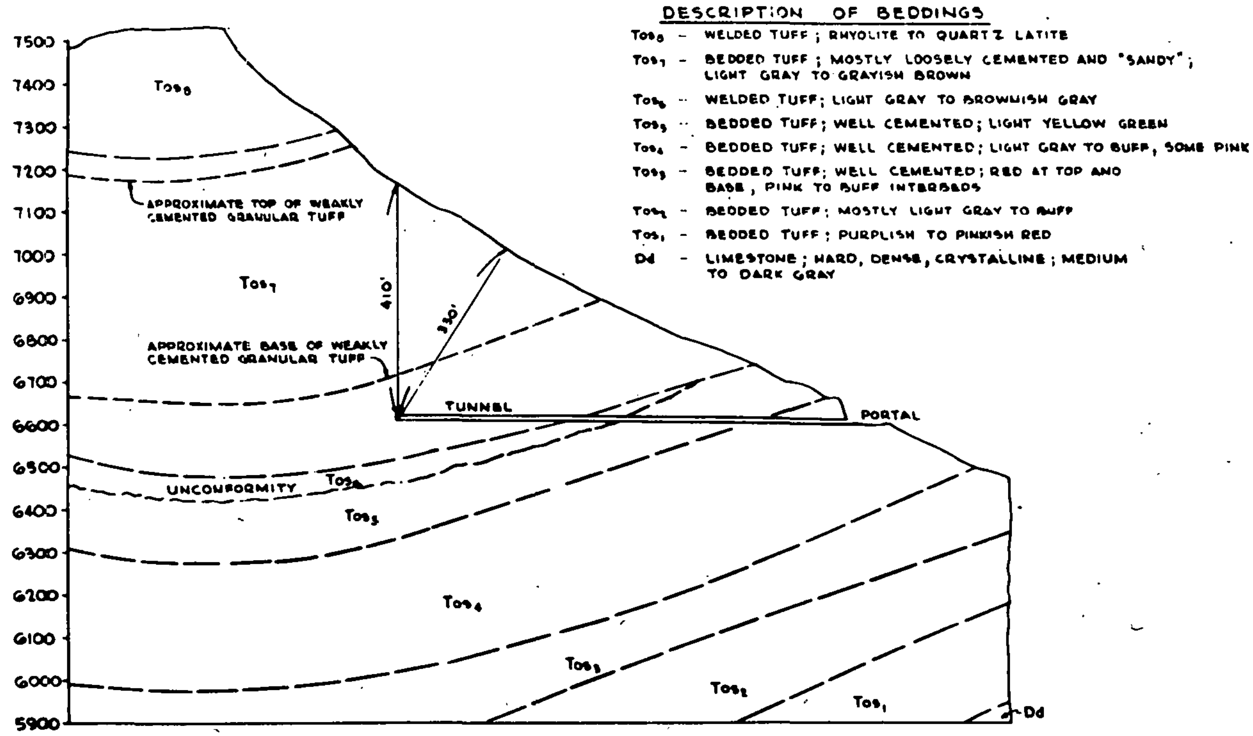

PROFILE OF TUNNEL SITE WITH GEOLOGIC CHARACTERISTICS "TAMALPAIS EVENT"

DRILL HOLES			
HOLE No.	SIZE	CASED	APPROX LENGTH
1	6"	6"	120'
2	8"	8"	118'
3	32"	3-8"	20'

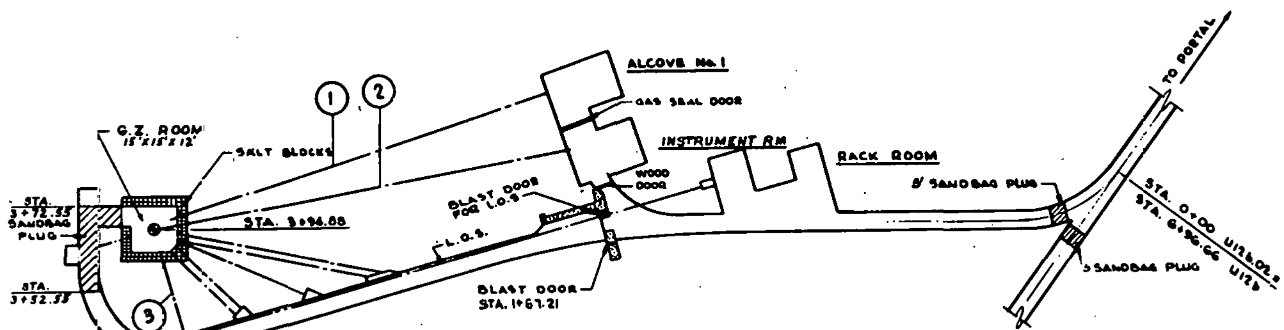

PLAN

MUL-7165

TUNNEL DRIFT U12b.02

Fig. 7, Appendix. Profile of Tamalpais site.

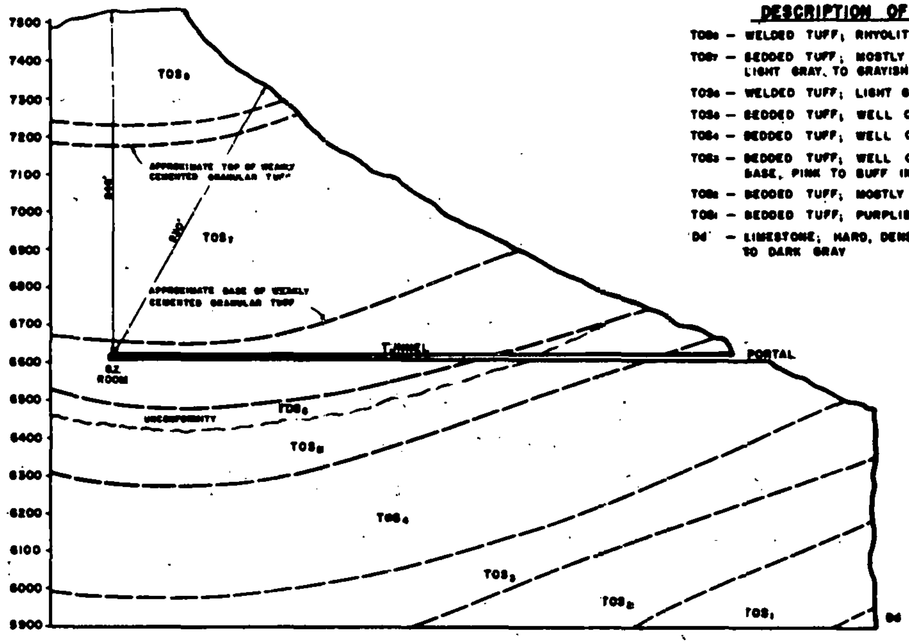

PROFILE OF TUNNEL SITE WITH GEOLOGIC CHARACTERISTIC "EVANS EVENT"

DESCRIPTION OF BEDDINGS

TOs9 – WELDED TUFF; RHYOLITE TO QUARTZ LATITE
TOs7 – BEDDED TUFF; MOSTLY ALL TUFFS ARE LOOSELY CEMENTED AND "SANDY" LIGHT GRAY TO GRAYISH BROWN
TOs6 – WELDED TUFF; LIGHT GRAY TO BROWNISH GRAY
TOs5 – BEDDED TUFF; WELL CEMENTED LIGHT YELLOW GREEN
TOs4 – BEDDED TUFF; WELL CEMENTED, LIGHT GRAY TO BUFF, SOME PINK
TOs3 – BEDDED TUFF; WELL CEMENTED, RED AT TOP AND BASE, PINK TO BUFF INTERBEDS
TOs2 – BEDDED TUFF; MOSTLY LIGHT GRAY TO BUFF
TOs1 – BEDDED TUFF; PURPLISH TO PINKISH RED
D4 – LIMESTONE; HARD, DENSE, CRYSTALLINE; MEDIUM TO DARK GRAY

DRILL HOLES

ALCOVE NO	SIZE	SIZE SEC. NO. 1	SIZE SEC. NO. 2	SIZE SEC. NO. 3	CASED	APPROX. LENGTH
1	8	\				29
2		12	12	12	6	115
3		12	6/12/18	12/28		115
4		18	18			115
5				12		115
6		18/12	30/12			115
7	6					28
8	6					28
9	8					28
10	8					28
11	10					17
12	10					17
14	4					15
15	6					15
16	4					19
17	6					19
18	4			1		19
19	8					19
20	4					19
21	6					19

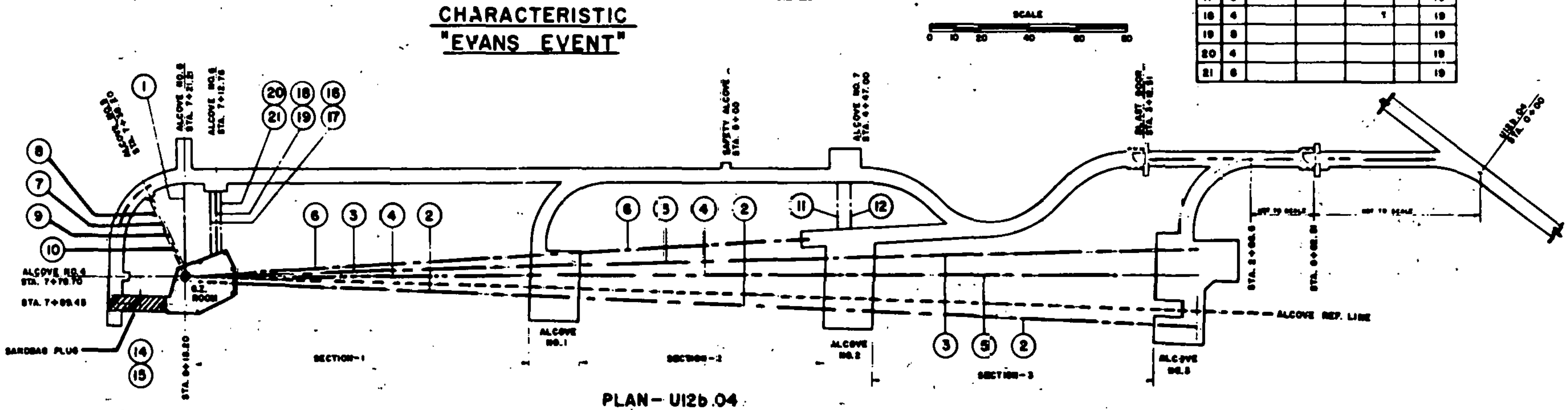

PLAN – U12b.04

MUL-7168

Fig. 8, Appendix. Profile of Evans site.

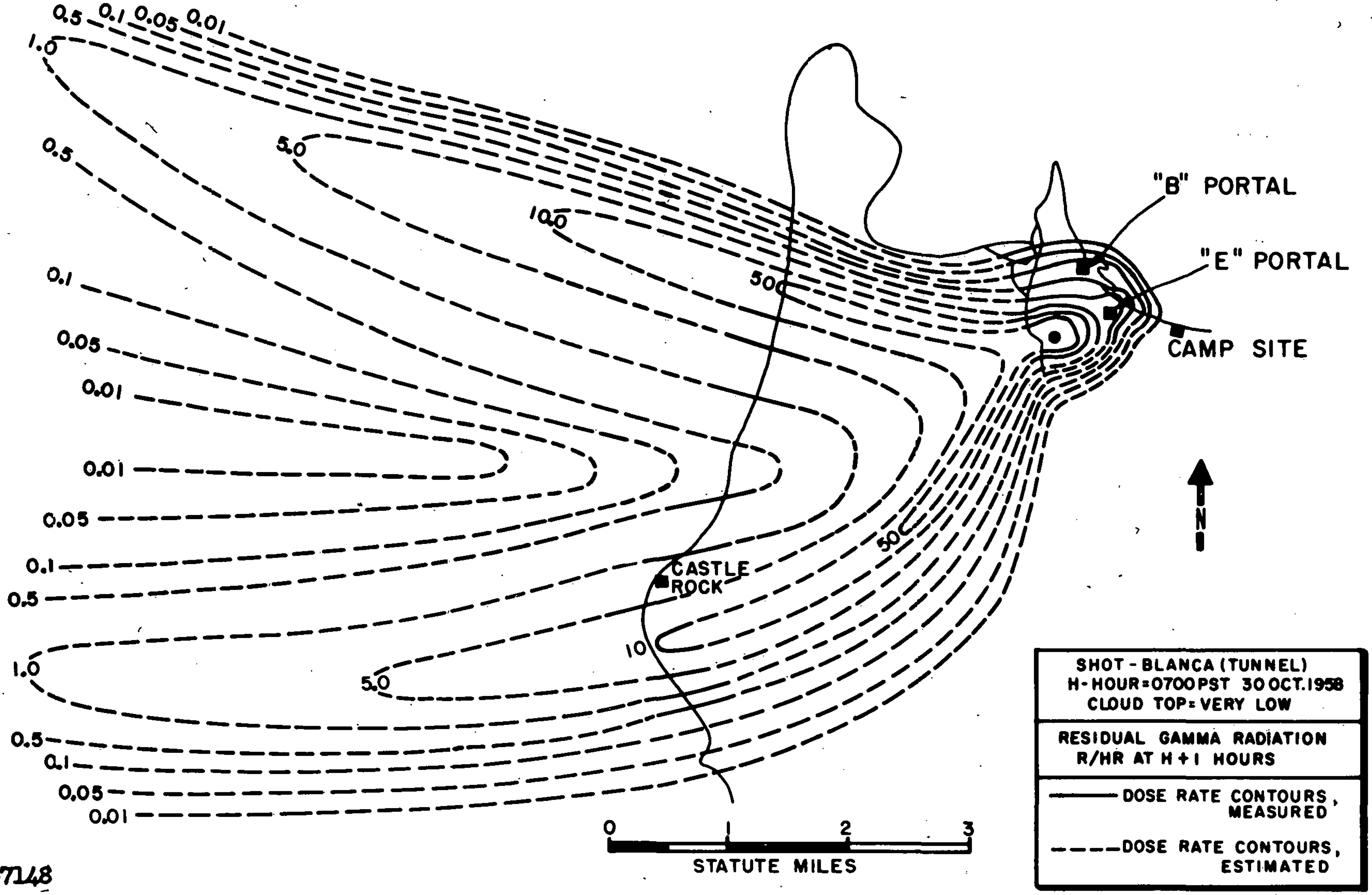

MUL-7148

Fig. 9, Appendix. Fallout pattern from Blanca Event.

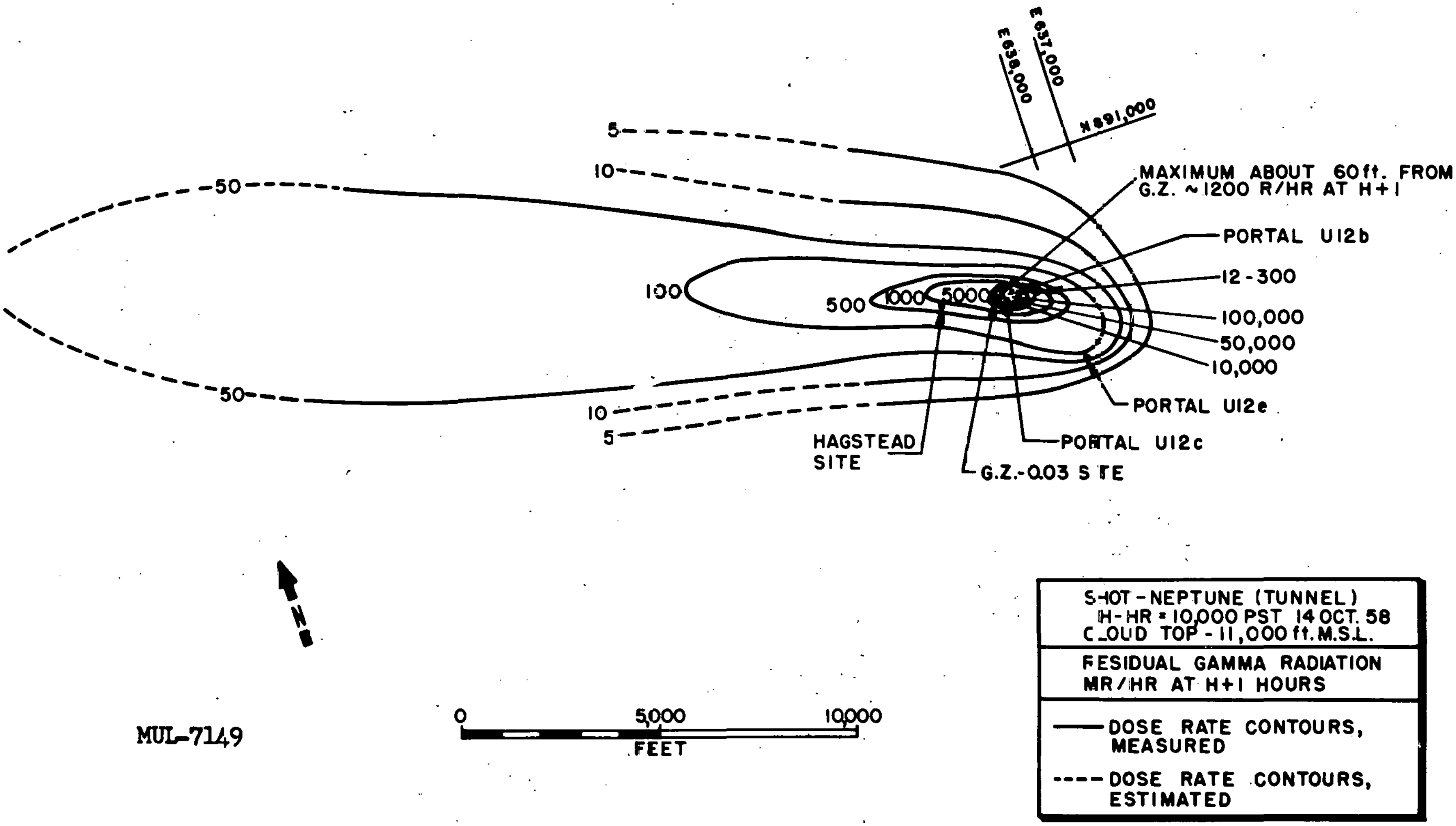

MUL-7149

Fig. 10, Appendix. Fallout pattern from Neptune Event.

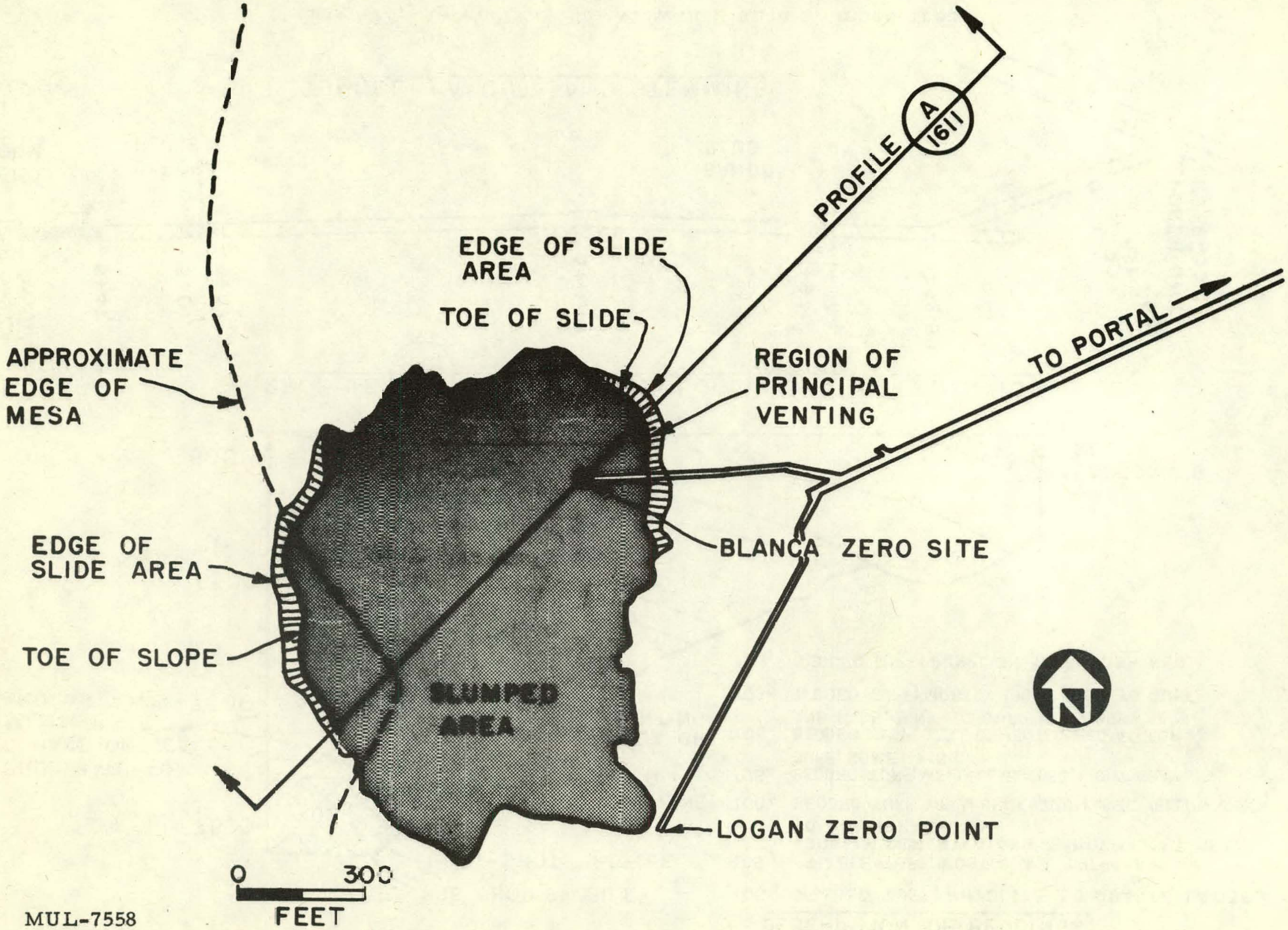

MUL-7558

Fig. 11, Appendix. Pre- and post-shot profiles of Blanca site.

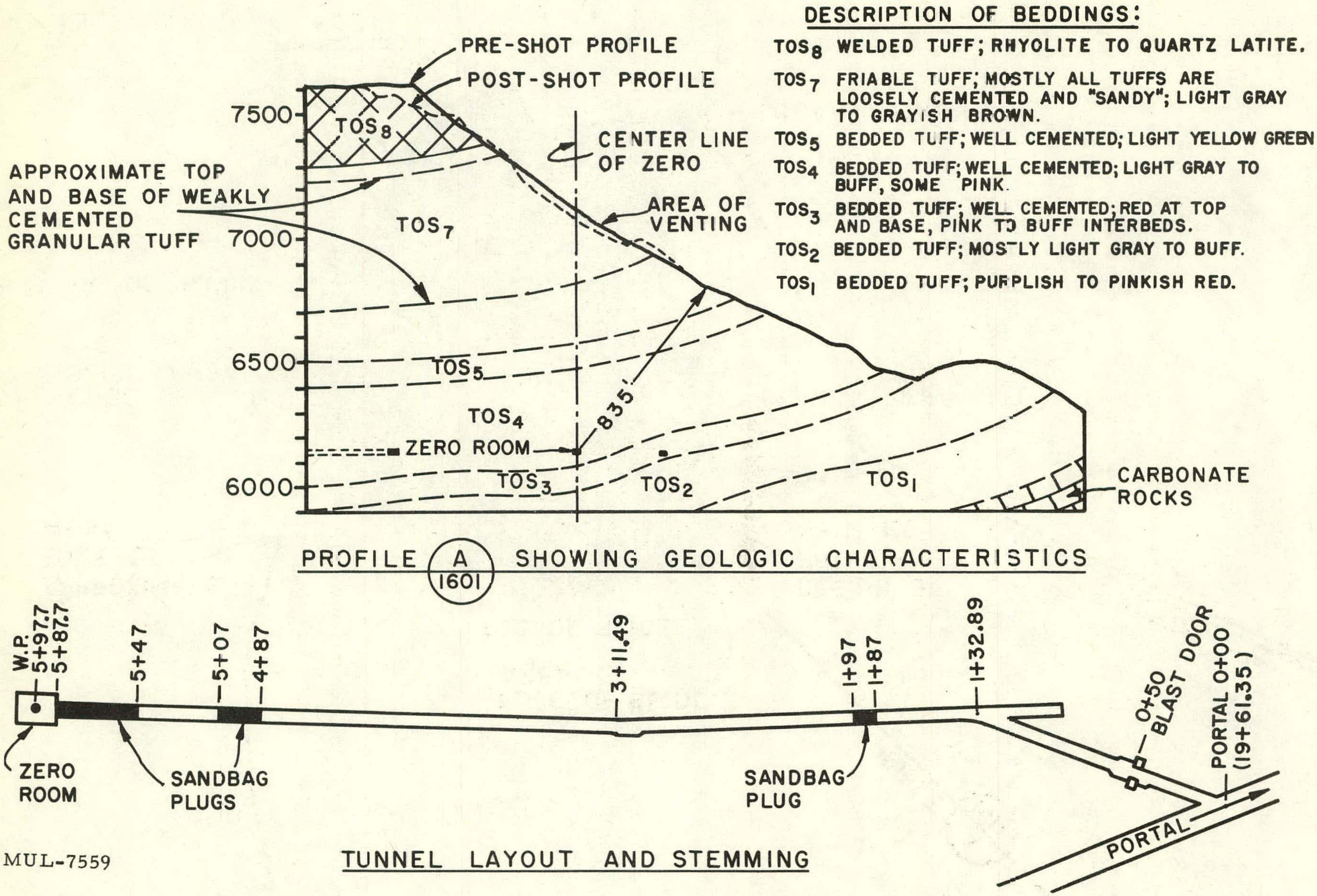

Fig. 12, Appendix. Plan view of Blanca slumped area.

LIST OF PREVIOUS PLOWSHARE AND/OR RELATED REPORTS

	Title
UCRL-4659	Deep Underground Test Shots.
UCRL-5026	Non-Military Uses of Nuclear Explosions.
UCRL-5124 Rev. I	Phenomenology of Contained Nuclear Explosions.
UCRL-5253	Industrial Uses of Nuclear Explosives.
UCRL-5257 Rev.	Peaceful Uses of Fusion.
UCRL-5281	Temperatures and Pressures Associated with the Cavity Produced by the Rainier Event.
UCRL-5457	Large Scale Excavation with Nuclear Explosives.
UCRL-5458	Mineral Resource Development by the Use of Nuclear Explosives.
UCRL-5538	Evaluation of the Ground Water Contamination Hazard from Underground Nuclear Explosions.
UCRL-5542	Properties of the Environment of Underground Nuclear Detonations at Nevada Test Site. Rainier Event.
UCRL-5623	Radioactivity Associated with Underground Nuclear Explosions.

/md

Printed in USA. Price $1.25. Available from the Office of Technical Services, Department of Commerce, Washington 25, D.C.